

**SYNTHESIS AND CHARACTERIZATION  
OF SULFONATED POLY(STYRENE-ISOPRENE-STYRENE):  
EFFECTS OF LINEAR VS BRANCHED MORPHOLOGY AND  
COUNTER-ION SUBSTITUTION**

by

Sully Mar Avilés Barreto

A thesis submitted in partial fulfillment of the requirements for the degree of

MASTER OF SCIENCE

in

CHEMICAL ENGINEERING

UNIVERSITY OF PUERTO RICO  
MAYAGÜEZ CAMPUS

2009

Approved by:

\_\_\_\_\_  
David Suleiman, PhD  
President, Graduate Committee

\_\_\_\_\_  
Date

\_\_\_\_\_  
L. Antonio Estévez, PhD  
Member, Graduate Committee

\_\_\_\_\_  
Date

\_\_\_\_\_  
Guillermo Colón, PhD  
Member, Graduate Committee

\_\_\_\_\_  
Date

\_\_\_\_\_  
Luis A. Rivera, PhD  
Representative of Graduate Studies

\_\_\_\_\_  
Date

\_\_\_\_\_  
David Suleiman, PhD  
Chairperson of the Department

\_\_\_\_\_  
Date

## Abstract

This investigation studied the resulting nanostructure of ionic membranes composed of sulfonated copolymers with thermoplastic and elastomeric blocks. Linear poly(styrene-isoprene-styrene) (L-SIS) and branched poly(styrene-isoprene) (B-SI), were sulfonated to various levels of ion exchange capacity (IEC). Since the sulfonation occurred in both the poly(styrene) (PS) blocks and the double bonds of the poly(isoprene) (PI) segments, the resulting sulfonated polymer lost the elastomeric component of the membranes; therefore, physical blends of sulfonated and unsulfonated L-SIS and B-SI were casted and analyzed. The resulting membranes were then characterized with several techniques including: elemental analysis (EA), thermogravimetric analysis (TGA), Fourier-transform infrared spectroscopy (FT-IR) and Small angle X-Ray scattering (SAXS). These techniques provided thermal and physical properties of the membranes, which allowed the comparison of the resulting morphologies and selectivities. Counter-ion substitution ( $Mg^{+2}$ ,  $Ca^{+2}$ ,  $Ba^{+2}$ ) was used to cross-linked the sulfonated polymers to create more selective membranes. Vapor permeabilities were measured at a temperature of 308 K using dimethyl methylphosphonate (DMMP), a chemical similar to Sarin Gas (GB), and water as permeates, in order to analyze the selectivity of the resulting membranes for chemical and biological protective clothing (CBPC). Results show a similar IEC to sulfonated poly(styrene-isobutylene-styrene) (SIBS), although the reaction kinetics was significantly faster due to the unsaturated bonds of the isoprene block. Selectivity values obtained from the permeability studies are not promising for the chemical and biological protective clothing application. However, lower sulfonation levels and blends of sulfonated/unsulfonated linear/branched resulted in unique morphologies capable of selective separations and significant differences were observed between linear and branched morphologies.

## Resumen

Durante esta investigación se estudiaron las nanoestructuras resultantes de membranas iónicas selectivas compuestas de polímeros sulfonados con bloques termoplásticos y elastoméricos. Se sulfonaron polímeros lineales y ramificados, poli(estireno-isopreno-estireno) y poli(estireno-isopreno), respectivamente, a diferentes niveles de capacidad de intercambio iónico. Debido a que la sulfonación ocurre tanto en los bloques del poli(estireno) como en los dobles enlaces de los segmentos del poli(isopreno), las membranas resultantes de los polímeros sulfonados pierden todas las propiedades elastoméricas, por lo tanto, se prepararon y analizaron membranas de mezclas físicas de polímeros sulfonados y sin sulfonar, lineales y ramificados. Todas las membranas caracterizaron utilizando diferentes técnicas como: análisis elemental, análisis termogravimétrico, espectroscopia de infrarrojo y dispersión de rayos X. Estas técnicas proveen propiedades térmicas y físicas de las membranas, lo que permitió la comparación de morfologías y selectividades. Se usó sustitución con iones de  $Mg^{+2}$ ,  $Ca^{+2}$  y  $Ba^{+2}$  para entrelazar y modificar los polímeros sulfonados y crear membranas más selectivas. Se realizaron medidas de permeabilidad en la fase gaseosa a una temperatura de 308 K, usando DMMP, un compuesto químico similar al gas tóxico Sarin, y agua como permeantes para analizar la selectividad de las membranas para la ropa protectora contra ataques químicos y biológicos. Los resultados muestran una capacidad de intercambio iónico similar a la del polímero sulfonado poli(estireno-isobutileno-estireno), a pesar de que la cinética de la reacción es mucho más rápida debido a los enlaces insaturados de los bloques del poli(isopreno). Los valores obtenidos para las selectividades de los estudios de permeabilidad no son prometedores específicamente para la aplicación de la ropa protectora contra ataques químicos y biológicos. Mezclas con bajos porcentajes de sulfonación de polímero lineal y ramificado, sulfonado y sin sulfonar, resultan en

morfologías únicas capaces de ser utilizadas en diferentes procesos selectivos de separación y diferencias significativas fueron observadas entre las dos morfologías, lineal y ramificada.

Copyright © 2009 by Sully Mar Avilés Barreto, MS Thesis, UPRM. All rights reserved. Printed in the United States of America. Except as permitted under the United States Copyright Act of 1976, no part of this publication may be reproduced or distributed in any form or by any means, or stored in a database or retrieval system, without the prior written permission of the publisher.

*To my parents José Luis Avilés (Güiso) and Sonia M. Barreto,*

*my sister Sonia L. Avilés Barreto,*

*and my love Jorge J. Torres (Ponce)...*

*"Desire is the key to motivation, but it's the determination and commitment to an unrelenting pursuit of your goal - a commitment to excellence - that will enable you to attain the success you seek." - Mario Andretti*

# Acknowledgements

Several persons contributed in one way or another during my graduate studies and research in the Chemical Engineering Department of the University of Puerto Rico at Mayagüez and I want to express my gratitude to all of them.

First, I wish to sincerely thank my advisor, **Dr. David Suleiman** for giving me the opportunity to work under his supervision and for all the support during these years. I appreciate all the personal and academic advises but specially his trust in me to do my research work.

Thanks to my **family** for all the support and unconditional love, especially to my sister, **Sonia** for been always with me when I need it. Thanks to my love, **Jorge “Ponce”**, for his patience, trust and love. Thanks to my friends for making the journey of the student life easier.

This work was performed with the support of the Department of Defense of the United States through grant number W911-NF-07-10244. Also, I would like to acknowledge the support of Prof. Danilo C. Pozzo, Ariangelis Ortíz and Gretselle F. Carreras.

Finally, but not less important, I would like to thank **God** for all the blessings and for giving me the strength and courage to continue and finish this goal.

# Table of Content

	<b>Page</b>
<b>List of Tables</b> .....	xi
<b>List of Figures</b> .....	xii
<b>List of Symbols</b> .....	xiv
<b>List of Appendices</b> .....	xvi
<b>1 Introduction</b>	
1.1 Motivation .....	1
1.2 Objectives .....	2
1.3 Overview of following Chapters .....	2
<b>2 Literature Review</b> .....	3
<b>3 Theoretical Background</b>	
3.1 Polymers .....	5
3.3.1 <i>Block Copolymers (BCs)</i> .....	5
3.2 Proton Exchange Membranes (PEMs) .....	6
3.2.1 <i>Proton Exchange Membrane Fuel Cell (PEMFC)</i> .....	7
3.3 Selectively Permeable Membranes (SPMs) .....	8
3.3.1 <i>Chemical and Biological Protective Clothing (CBPC)</i> .....	9
3.4 Thermoplastic Elastomers (TPEs) .....	9
3.4.1 <i>Nafion<sup>®</sup></i> .....	10
3.4.2 <i>Poly(styrene-isobutylene-styrene) (SIBS)</i> .....	11
3.5 Separation Processes .....	11
<b>4 Experimental Methods</b>	
4.1 Materials .....	13
4.2 Equipment .....	13
4.3 Sulfonation .....	14
4.4 Blends .....	17
4.5 Membrane Casting .....	19
4.6 Cation Substituted Cross-linked Membranes .....	20
4.7 Characterization Techniques .....	20
4.7.1 <i>Elemental Analysis (EA)</i> .....	20
4.7.2 <i>Thermogravimetric Analysis (TGA)</i> .....	21
4.7.3 <i>Water Swelling</i> .....	22
4.7.4 <i>Permeability</i> .....	22
4.7.4.1 <i>Theory</i> .....	22
4.7.4.2 <i>Permeability Experiments</i> .....	24

4.7.5	<i>FT-IR Spectroscopy</i> .....	26
4.7.5.1	<i>Stretching and Bending Vibrations</i> .....	27
4.7.5.2	<i>Infrared Spectroscopy of Organic Sulfur Compounds</i> .....	28
a.	<i>Thiols</i> .....	28
b.	<i>Sulfoxides and Sulfites</i> .....	29
c.	<i>Sulfones, Sulfonates and Sulfates</i> .....	29
4.7.6	<i>Small Angle X-Ray Scattering (SAXS)</i> .....	29
4.7.6.1	<i>SAXS Instrument Resolution</i> .....	30
4.7.7	<i>Scanning Electron Microscope (SEM)</i> .....	31
<b>5</b>	<b>Results and Discussions</b>	
5.1	Sulfonation Analysis .....	32
5.2	Degradation Temperatures .....	33
5.2.1	<i>Blends</i> .....	36
5.3	Water Swelling .....	40
5.4	Permeability .....	43
5.4.1	<i>Permeability Analysis</i> .....	43
5.4.2	<i>Selectivity</i> .....	46
5.5	FT-IR Spectroscopy .....	48
5.6	Small Angle X-Ray Scattering (SAXS) .....	53
5.6.1	<i>SAXS Form Factor</i> .....	53
5.6.2	<i>SAXS Structure Factor</i> .....	53
5.7	Scanning Electron Microscope (SEM) .....	61
<b>6</b>	<b>Conclusions and Recommendations</b> .....	63
<b>7</b>	<b>References</b> .....	64

## Appendices

Appendix A		
A.1	Sulfonation Reaction Stoichiometric Calculations .....	68
Appendix B		
B.1	Elemental Analysis Results .....	69
B.2	Sulfonation Level Calculations .....	70
Appendix C		
C.1	Water Swelling Data for sulfonated and cross-linked Blend Membranes .....	71
Appendix D		
D.1	DMMP Vapor Transport Data .....	76
D.2	Water Vapor Transport Data .....	81
Appendix E		
E.1	SAXS curves used to calculate the Bragg distance .....	87

# List of Tables

<b>Tables</b>	<b>Page</b>
Table 1. Separation Processes using polymer membranes . . . . .	12
Table 2. SIS/SI Sulfonation levels . . . . .	31
Table 3. Blends Sulfonation Levels . . . . .	32
Table 4. Degradation Temperatures for sulfonated/unsulfonated linear/branched SIS . . . . .	35
Table 5. Degradation Temperatures for linear and branched blends . . . . .	38
Table 6. Bragg distance for linear and branched blends . . . . .	61

# List of Figures

<b>Figures</b>	<b>Page</b>
Figure 1. Proton Exchange Membrane for Methanol Fuel Cells Application . . . . .	8
Figure 2. Schematic Diagram for the Chemical and Biological Protective Clothing (CBPC) Application . . . . .	9
Figure 3. Nafion <sup>®</sup> Chemical Structure with Sulfonic Groups . . . . .	10
Figure 4. SIBS Chemical Structure . . . . .	11
Figure 5. Schematic Diagram of the equipment for the sulfonation reaction . . . . .	14
Figure 6. Sulfonation Reaction for the SIS/SI polymers . . . . .	15
Figure 7. SIBS Chemical Structure with Sulfonic Groups . . . . .	15
Figure 8. Chemical Modification of PS Blocks in SIBS Polymer . . . . .	16
Figure 9. Chemical Morphologies after sulfonation . . . . .	17
Figure 10. Polymers Elastomeric Properties . . . . .	18
Figure 11. Crystals Ordered Arrangements for polymers . . . . .	18
Figure 12. Schematic Diagram for Vapor Permeation . . . . .	25
Figure 13. Chemical Structures of DMMP and Sarin toxic Agent . . . . .	26
Figure 14. Symmetric and asymmetric stretching vibrations for the SO <sub>2</sub> molecule . . . . .	27
Figure 15. Bending vibration for the SO <sub>2</sub> molecule . . . . .	27
Figure 16. Thermogravimetric Analysis (TGA) for L-SIS-0.0 . . . . .	34
Figure 17. Thermogravimetric Analysis (TGA) for B-SI-0.0 . . . . .	35
Figure 18. Thermogravimetric Analysis (TGA) for L-SIS-37.8 . . . . .	35
Figure 19. Thermogravimetric Analysis (TGA) for B-SI-63.0 . . . . .	36
Figure 20. Thermogravimetric Analysis (TGA) for M-LL-SIS-9.7 . . . . .	37
Figure 21. Thermogravimetric Analysis (TGA) for M-LL-SIS-14.3 . . . . .	38
Figure 22. Thermogravimetric Analysis (TGA) for M-BL-SIS-12.6 . . . . .	38
Figure 23. Thermogravimetric Analysis (TGA) for M-BL-SIS-23.3 . . . . .	39

Figure 24. Linear vs. Branched effects on Water Swelling Studies .....	40
Figure 25. Cations Effect on Water Swelling Studies for M-BL-SIS-9.7 Blend .....	41
Figure 26. Cations Effect on Water Swelling Studies for M-BL-SIS-14.3 Blend .....	41
Figure 27. Cations Effect on Water Swelling Studies for M-BL-SIS-12.6 Blend .....	42
Figure 28. Cations Effect on Water Swelling Studies for M-BL-SIS-23.3 Blend .....	42
Figure 29. VTR of Water in Vapor Transfer Studies for Blend Membranes .....	44
Figure 30. $P_{\text{eff}}$ of Water in Vapor Transfer Studies for Blend membranes .....	44
Figure 31. VTR of DMMP in Vapor Transfer Studies for Blend Membranes .....	45
Figure 32. $P_{\text{eff}}$ of DMMP in Vapor Transfer Studies for Blend membranes .....	45
Figure 33. Selectivity between Water and DMMP Vapor Transport Studies .....	47
Figure 34. FT-IR Spectrums for linear blend M-LL-SIS-9.7 and unsulfonated L-SIS-0.0 ...	49
Figure 35. FT-IR Spectrums for branched blend M-BL-SIS-12.6 and unsulfonated B-SI-0.0 .....	50
Figure 36. FT-IR Spectrums for branched blend M-LL-SIS-9.7 and cross-linked with $\text{Ca}^{+2}$ , $\text{Ba}^{+2}$ , $\text{Mg}^{+2}$ .....	51
Figure 37. FT-IR Spectrums for branched blend M-BL-SIS-12.6 and cross-linked with $\text{Ca}^{+2}$ , $\text{Ba}^{+2}$ , $\text{Mg}^{+2}$ .....	52
Figure 38. Domains of a particle form factor .....	54
Figure 39. Logarithmic SAXS Profile for B-SI-106.1 and B-SI-14.09 .....	55
Figure 40. Logarithmic SAXS Profile for L-SIS-93.2 and L-SIS-8.71 .....	56
Figure 41. SAXS Profile for blends M-LL-SIS-9.7, M-LL-SIS-9.7-Ba, M-LL-SIS-9.7-Ca and M-LL-SIS-9.7-Mg .....	57
Figure 42. SAXS Profile for blends M-LL-SIS-12.6, M-LL-SIS-12.6-Ba, M-LL-SIS-12.6-Ca and M-LL-SIS-12.6-Mg .....	58
Figure 43. SAXS Profile for blends M-BL-SIS-12.6, M-BL-SIS-12.6-Ba, M-BL-SIS-12.6-Ca and M-BL-SIS-12.6-Mg .....	59
Figure 44. SAXS Profile for blends M-BL-SIS-23.3, M-BL-SIS-23.3-Ba, M-BL-SIS-23.3-Ca and M-BL-SIS-23.3-Mg .....	60
Figure 45. Range of Applicability of different Characterization Techniques .....	62
Figure 46. SEM images of the nanostructured membranes .....	62

# List of Symbols

## Symbols

CBPC	Chemical and biological protective clothing
SIBS	Poly(styrene-isobutylene-styrene)
SIS	Poly(styrene-isoprene-styrene)
SI	Poly(styrene-isoprene)
IEC	Ion exchange capacity
SPM	Selectively permeable membrane
BC	Block copolymer
PEM	Proton exchange membrane
PEMFC	Proton exchange membrane fuel cell
TPE	Thermoplastic elastomer
PS	Poly(styrene)
PIB	Poly(isobutylene)
PI	Poly(isoprene)
L-SIS	Linear poly(styrene-isoprene-styrene)
B-SI	Branched poly(styrene-isoprene)
W	Weight
V	Volume
EA	Elemental analysis
MgCl <sub>2</sub>	Magnesium Chloride
CaCl <sub>2</sub>	Calcium chloride
BaCl <sub>2</sub>	Barium chloride
TGA	Thermogravimetric analysis
DMMP	Dimethyl methylphosphonate
mL	Mililiters
GP	Sarin nerve gas
FT-IR	Fourier transform infrared spectroscopy
ATR	Attenuated total reflectance
SAXS	Small angle X-ray scattering
hr	Hours
°C	Degree Celsius
T <sub>g</sub>	Degradation temperature

wt %	Weight percent
$J_A$	Diffusion flux
$D_{AB}$	Diffusivity
$dC_A/dx_A$	Concentration gradient
VTR	Vapor transfer rate
t	Time
A	Cross-sectional area
$P_{eff}$	Effective permeability
L	Membrane thickness
$\Delta C_i$	Change in permeant concentration
MW	Molecular weight
R	Gas constant
T	Temperature
K	Kelvin
$P_{i1}$	Partial pressure of the permeant inside the vial
$P_{i2}$	Partial pressure of the permeant outside the vial
$P_i^{vap}$	Vapor pressure
$P_{N_2}$	Nitrogen partial pressure
$P_{eff\ water}$	Water effective permeability
$P_{eff\ DMMP}$	Dimethyl methylphosphonate effective permeability
D	Diameter
$P^{sat}$	Saturation pressure
DMA	Dynamic mechanical analysis
TEM	Transmission electron microscopy
$d_{Bragg}$	Bragg distance
$q_{Bragg}$	Bragg length scattering vector
$D_{min}$	Minimum resolution diameter
$D_{max}$	Maximum resolution diameter
$q_{min}$	Minimum length scattering vector
$q_{max}$	Maximum length scattering vector
$d_{min}$	Minimum lattice spacing or distance
$d_{max}$	Maximum lattice spacing or distance

# List of Appendices

	Page
<b>Appendix A</b>	
A.1 Sulfonation Reaction Stoichiometric Calculations .....	68
<b>Appendix B</b>	
B.1 Elemental Analysis Results .....	69
B.2 Sulfonation Level Calculations .....	70
<b>Appendix C</b>	
C.1 Water Swelling Data for sulfonated and cross-linked Blend Membranes .....	71
<b>Appendix D</b>	
D.1 DMMP Vapor Transport Data .....	76
D.2 Water Vapor Transport Data .....	81
<b>Appendix E</b>	
E.1 SAXS curves used to calculate the Bragg distance .....	87

# 1 Introduction

## 1.1 Motivation

Security and protection are two important things for people in general and in particular for the US military forces, in which they have to protect their own soldiers from any chemical or biological attack. After the 911 terrorist attack, security became the most important issue for the United States. For that reason the development and implementation of new and more efficient alternatives for chemical and biological protective clothing (CBPC) is of outmost importance. Linear poly(styrene-isobutylene-styrene) (SIBS) was the typical material used for that specific application and investigations have demonstrated that increasing sulfonic groups in the polymer matrix results in increased proton transport and water uptake [1]. Poly(styrene) has been known for years as commodity plastic with many desired properties, such as excellent chemical resistance, good environmental stress crack resistance, easy processability and moderate cost [2]. The proposed block copolymers, linear poly(styrene-isoprene-styrene) (L-SIS) and branched poly(styrene-isoprene) (B-SI) are thermoplastic elastomers and sulfonated at high ion exchange capacities (IEC) are expected to act like ionomers forming ion-rich and ion-poor domains with the sulfonic groups creating nanochannels that allow water vapor to permeate [3] providing a more pleasant environment for soldiers. The purpose of this investigation is to analyze the sulfonated polymers in order to create selectively permeable membranes (SPMs) and obtain different morphologies and high selectivity with the cation cross-linking to produce an efficient alternative for the chemical and biological protective clothing.

## 1.2 Objectives

- ❖ Synthesize and characterize sulfonated linear Poly(Styrene-Isoprene-Styrene) and branched Poly(Styrene-Isoprene) polymers.
- ❖ Analyze different sulfonated polymers in order to obtain different morphologies and high selectivity.
- ❖ Understand the complex orientation and the relaxation behavior of other polymers and develop an alternative to the chemical and biological protective clothing (CBPC).
- ❖ Develop low-cost selectively permeable membranes (SEMs).

## 1.3 Overview of following Chapters

Motivation and objectives of this research were presented in Chapter 1. Chapter 2 presents some of the literature review related to the experiments. Chapter 3 focuses on the theoretical background of the investigation. Chapter 4 deals with the experimental methods, materials, procedures, and the characterization techniques used to analyze the selective materials. Chapter 5 presents the results and the data analysis of each experiment and characterization. Finally, conclusions and recommendations are presented in Chapter 6.

## 2 Literature Review

Historically, many investigations have been conducted in which polymers are modified chemically and structurally and characterized for different types of applications. Regarding direct methanol fuel cells, researchers have focused on developing more efficient techniques [4 – 16].

Silva and co-workers et al. [17] studied the behavior of proton exchange membranes for direct methanol fuel cells. Using a one-dimensional steady state mathematical model, they simulated and analyzed the proton conductivity and the critical properties concerning the methanol crossover problem.

Yildirim et al. [18] worked with different types of Nafion to understand the effect of impregnation of an ion-conductive polymer membrane to the fuel cell performance. Membranes were characterized with respect to their water swelling degree, methanol crossover and proton conductivity.

During these years other sulfonated polymers have been used and studied for fuel-cell applications. Jung and co-workers et al. [19] studied the transport of methanol and protons through sulfonated polymer membranes, specifically sulfonated poly(styrene) and sulfonated poly(2,6-dimethyl-1,4-phenylene oxide). FT-IR spectroscopy was used to detect sulfonic groups in the polymer matrix and thermogravimetric analysis was used to study the thermal stability of the sulfonated polymers.

All these proton exchange membranes and other selectively permeable membranes are used in the Army Research Lab to develop and improve the chemical and biological protective clothing application. In 2001, Crawford et al. [20] studied the structure and properties of poly(styrene-isobutylene-styrene) tri-block copolymers. Dynamic mechanical analysis (DMA),

small angle X-ray scattering (SAXS) and transmission electron microscopy (TEM) were the characterization techniques used to analyze the morphology of this sulfonated polymer. They concluded that the modified tri-block copolymer showed distinctly different thermal and mechanical characteristics than unmodified copolymer and that sulfonic groups increase properties and the morphology characteristics of the polymers.

Suleiman and co-workers of the Army Research Lab et al. [21] worked on the thermogravimetric characterization of sulfonated poly(styrene-isobutylene-styrene) block copolymers. They studied the degradation temperature and the infrared spectroscopy behavior of the polymer at different sulfonation levels. Their study revealed better thermal stability in sulfonated polymers and the same degradation temperature regardless of the sulfonation level.

Among these years, investigators of the Army Research Lab studied the breathability, selectivity and the viscoelastic and transport properties of selected materials for the protective clothing application. In these investigations counter ion-substitution were performed to increase the selectivity of those materials and morphology arrangements were confirmed at different sulfonation levels [22-23].

In different publications, other types of experiments were performed to select which is the better material for the chemical and biological protective clothing. Jonquieres et al. [24] reviewed the literature on permeability of block copolymers to vapors and liquids for 40 years. Permeability of block copolymers is an important feature for a broad range of applications including packaging, bio-materials (e.g. for controlled release or encapsulating membranes), barrier materials, high performance impermeable breathable clothing and membrane separation processes.

## 3 Theoretical Background

### 3.1 Polymers

Polymers are made up of many molecules all strung together to form really long chains. Polymers are substances whose molecules have high molar masses and are composed of a large number of repeating units. There are both naturally occurring and synthetic polymers. Among naturally occurring polymers are proteins, starches, cellulose, and latex. Synthetic polymers are produced commercially on a very large scale and have a wide range of properties and uses. The materials commonly called plastics are all synthetic polymers. Polymers act depends on what kinds of molecules they are made up of and how they are put together. Things that are made of polymers look, feel, and act depending on how their atoms and molecules are connected. Today, polymeric materials are used in nearly all areas of daily life and their production and fabrication are major worldwide industries.

#### 3.1.1 Block Copolymers (BCs)

A block copolymer (BC) is a special type of polymer in which each molecule consists of two or more segments of simple polymers joined in some arrangement. Polymers can be divided in homopolymers, in which each molecule is composed of the same type of monomer, and copolymers, in which each molecule is composed of more than one type of monomer. Copolymers are divided into random and block types. In block copolymers, the different monomers are organized into distinct segments, or blocks. Block copolymers are further classified by the number of blocks each molecule contains, and how they are arranged.

Block copolymers with two, three, and more blocks are called diblocks, triblocks, and multiblocks, respectively. Some arrangements are linear, in which the blocks are connected end-to-end, and star, in which all of the blocks are connected via one of their ends at a single junction. More complicated arrangements are possible, like branched. Most applications of block copolymers are stemming from their ability to form microdomains in solution and in bulk. Current applications of block copolymers include thermoplastic elastomers and compatibilization of polymer blends. The potential uses of block copolymers in emerging technologies like nanotechnology, nanolithography, photonics and controlled drug delivery are enormous. The relationships between the chemical structure of block copolymers and their physical properties and their present and future applications are highlighted [25].

### **3.2 Proton Exchange Membranes (PEMs)**

Proton exchange membranes (PEMs) are semipermeable membranes generally made from ionomers. A semi-permeable membrane is a very thin film that lets some materials pass through while others remain inside. More specifically, a PEM will only allow certain molecules or ions to pass through it by diffusion. Ionomers are copolymers with both nonionic repeat units and ion containing repeat units with electric charge. The membranes made with ionomers are called specifically ion-selective membranes. These ion-selective membranes work by letting water pass through and not the metal ions. Polymers used for PEMs must exhibit high proton conductivities and a good resistance to the high-temperature, humid and oxidative environment of a fuel cell [26].

### **3.2.1 Proton exchange membrane fuel cell (PEMFC)**

A proton exchange membrane serves as a solid electrolyte in a fuel cell, separating the anode (hydrogen or methanol) from the cathode (oxygen/air) compartments [27-28]. Proton exchange membranes for fuel cells are designed to conduct protons while being impermeable to gases such as oxygen or hydrogen. Proton exchange membrane fuel cells (PEMFCs) are the most attractive power sources for transport, stationary, and portable applications, because of their high power density and high energy conversion efficiency as well as low pollution levels [29-31].

One of the most important issues for the development of PEMFCs concerns polymer electrolyte membranes, for which several specific and demanding properties are required; good chemical and electrochemical stability, mechanical strength, high proton conductivity, low gas ( $H_2$ ,  $O_2$ , or methanol) permeability, and a low price [32]. Figure 1 shows how a proton exchange membrane works for the methanol fuel cell application. In general, the protons pass through the membrane, while electrons were refused creating an electrical current to produce electricity. Finally, an external flow of oxygen was used to obtain water.

# Methanol Fuel cell Membranes

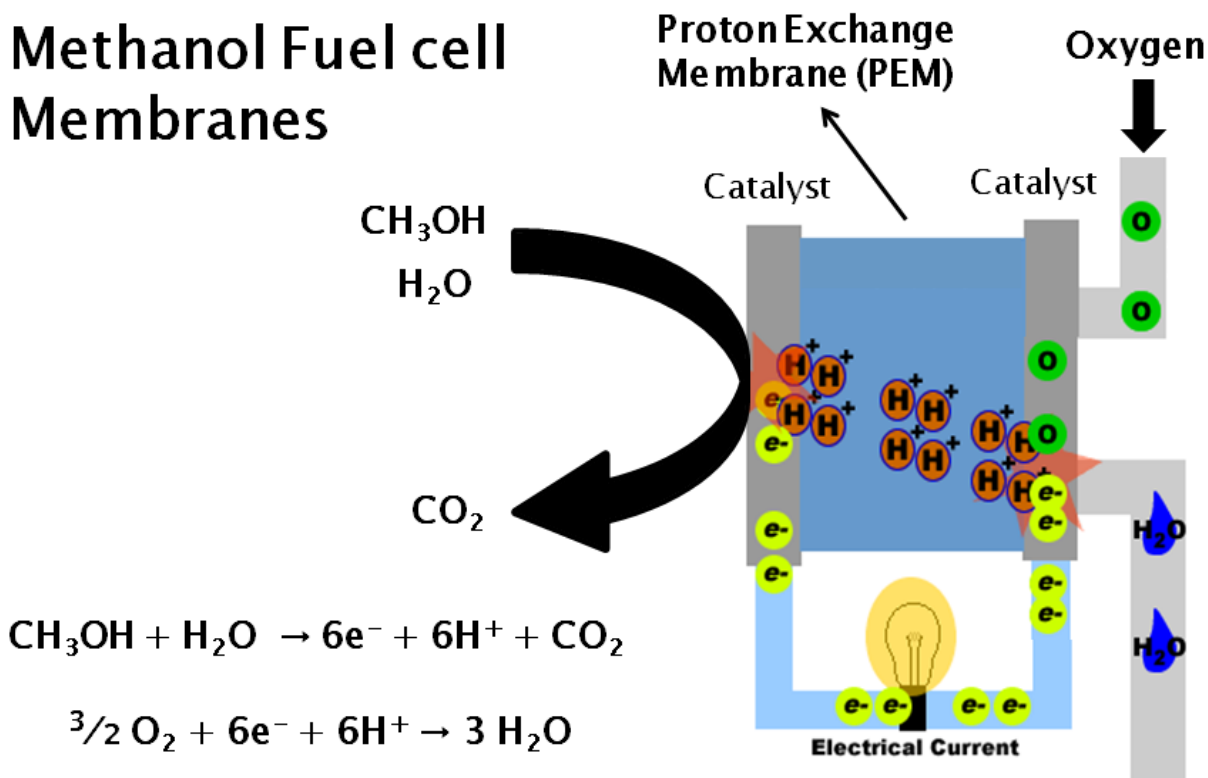


Figure 1. Proton Exchange Membrane for Fuel Cells Application

### 3.3 Selective Permeable Membranes (SPMs)

Years ago, most of the chemical and biological protective clothing used by the military forces was based on the use of activated charcoal, which is carbon that has been treated with oxygen to open up hundreds of thousands of pores inside of it. This material acts like a filter providing protection to soldiers but is quite heavy and uncomfortable. For that reason, selective permeable membranes (SPMs) have been developed as a lighter material in textile systems.

### **3.3.1 Chemical and Biological Protective Clothing (CBPC)**

The chemical and biological protective clothing serves like protection to the human body and as an effective barrier to toxic agents and hazardous chemicals while allowing an agreeable degree of moisture. Figure 2 shows how the concept of the selective permeable membrane is implemented in the chemical and biological protective clothing application.

**Figure 2. Schematic Diagram for the Chemical and Biological Protective Clothing (CBPC) Application**

### **3.4 Thermoplastic Elastomers (TPEs)**

Thermoplastic elastomers (TPEs) offer the main advantages of two types of polymeric materials: elastomeric behavior at room temperature and thermoplastic behavior at processing

temperatures. This dual behavior is obtained because the morphology consists of small rubber particles dispersed in a continuous thermoplastic matrix [33]. TPE are copolymers or a physical mix of polymers (usually a plastic and a rubber) which consist of materials with both thermoplastic and elastomeric properties. Elastomers are excellent for chemical processes requiring flexibility, strength, and durability. Thermoplastics are high molecular weight polymers in which chains are associated to weak Van der Waals forces, stronger dipole-dipole interactions and hydrogen bonding or stacking of aromatic rings which is the case of poly(styrene).

### 3.4.1 Nafion<sup>®</sup>

DuPont's Nafion is the most frequently used commercial PEM for Fuel Cells because is a good proton conductor, a good thermal stability and a good solvent resistant. Nafion's unique ionic properties are a result of incorporating perfluorovinyl ether groups terminated with sulfonate groups onto a tetrafluoroethylene (Teflon) backbone [34] as show in Figure 3.

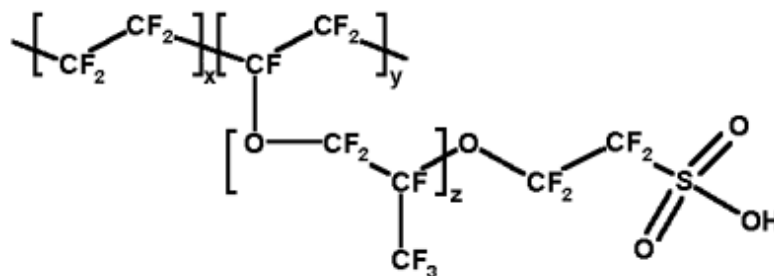


**Figure 3. Nafion<sup>®</sup> Chemical Structure with Sulfonic Groups**

### 3.4.2 Poly(styrene-isobutylene-styrene) (SIBS)

SIBS is the typical material used for the chemical and biological protective clothing (CBPC) application because blocks toxic agents but cause fatigue and exhaustion in the soldiers [35]. SIBS is a tri-block copolymer composed of poly(styrene) and poly(isobutylene). Figure 4 shows the chemical structure of SIBS polymer. The poly(styrene) (PS) block provides stability and rigidity to the polymer and is the glassy segment of the tri-block copolymer. The PS blocks are modified chemically to enable water transport. The poly(isobutylene) (PIB) is the segment that provides the elastomeric and barrier properties to the polymer.

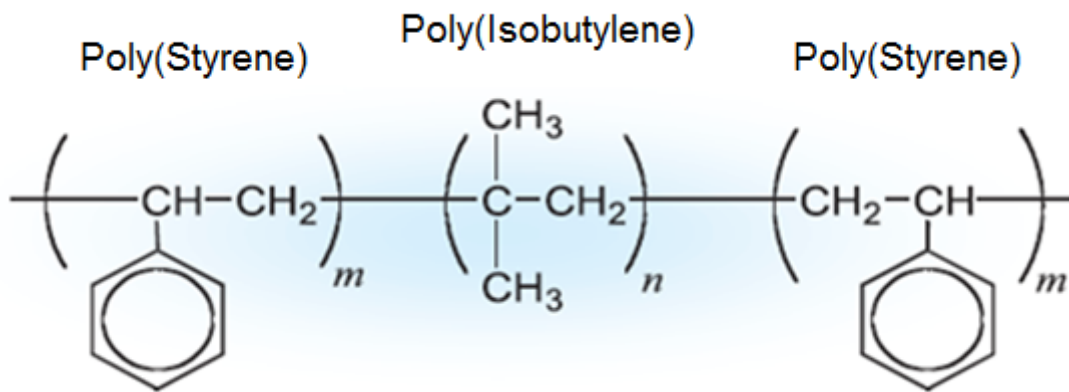


Figure 4. SIBS Chemical Structure

### 3.5 Separation Processes

Table 1 presents different separation processes in which membranes made from polymers are used for essential part of the separations. The most important of these processes include: (i) microfiltration and ultrafiltration for purification of aqueous streams, concentration and recovery

of valuable products; (ii) reverse osmosis for the production of demineralized or potable water; (iii) electrodialysis for the concentration or removal of dissolved ions; (iv) gas separation for splitting gas streams, removal or recovery of specific gases; (v) pervaporation for separation and concentration of liquid mixtures, especially of aqueous-organic azeotropes [36].

**Table 1. Separation Processes using Polymer Membranes**

<b>Separation Process</b>	<b>Membrane Type</b>	<b>Membrane Material</b>	<b>Applications</b>
Microfiltration	Symmetric microporous	Polyvinylidene difluoride (PVDF), Polyamides, Polysulfone, PTFE	Sterile filtration, Clarification
Ultrafiltration	Asymmetric microporous	Polysulfone, Polypropylene, Nylon 6, PTFE, PVC, Acrylic Copolymer	Separation of macromolecular solutions
Reverse Osmosis	Asymmetric skin-type	Polymers, Cellulosic acetate, Aromatic Polyamide	Separation of salts and microsolute from solutions
Electrodialysis	Cation and anion exchange membrane	Sulfonated cross-linked polystyrene	Desalting of ionic solutions
Gas Separation	Asymmetric homogeneous polymer	Polymers & copolymers	Separation of gas mixtures
Pervaporation	Asymmetric homogenous polymer	Polyacrylonitrile, Polymers	Separation of azeotropic mixtures
Nanofiltration	Thin-film membranes	Cellulosic Acetate and Aromatic Polyamide	Removal of hardness and Desalting

## 4 Experimental Methods

### 4.1 Materials

Linear poly(styrene-isoprene-styrene) triblock copolymer and branched poly(styrene-isoprene) diblock copolymer were provided by Kraton Polymers with the reported properties of 30%PS and 0.94 specific gravity. Other chemicals used in this study were as follows: Methylene Chloride (Fisher Scientific, Stabilized HPLC Grade), Acetic Anhydride (Aldrich Chemical Company, Inc., 99+%), Sulfuric Acid (Sigma-Aldrich, 95-98%) and Methanol (Fisher Scientific, Optima<sup>\*</sup>, 99.9%) for the sulfonated polymer synthesis; Toluene (Fisher Scientific, Optima<sup>\*</sup>, 99.8%), Hexyl Alcohol (Aldrich, Reagent Grade, 98%) for the membrane casting; Dimethyl Methyl-phosphonate (DMMP) (Aldrich, 97%) for the vapor permeability studies; Magnesium Chloride (Sigma Aldrich, anhydrous, powder, 99.99%), Calcium Chloride (Sigma Aldrich, anhydrous, powder, 99.99%), Barium Chloride (Sigma Aldrich, anhydrous, powder, 99.99%) for the membrane cross-linking; water solution for HPLC (Sigma-Aldrich) for the water swelling experiments and deionized water.

### 4.2 Equipment

The sulfonation reaction was carried out in a batch reactor (see Figure 5) and the general equipment consists of a flask with three orifices, a condenser with an ice bath and a thermometer to monitor the temperature of the exothermic reaction. The condenser and the cooling bath were used to prevent evaporation of the volatile solvents of the reaction, specifically the methylene chloride which has a boiling point of 40°C.

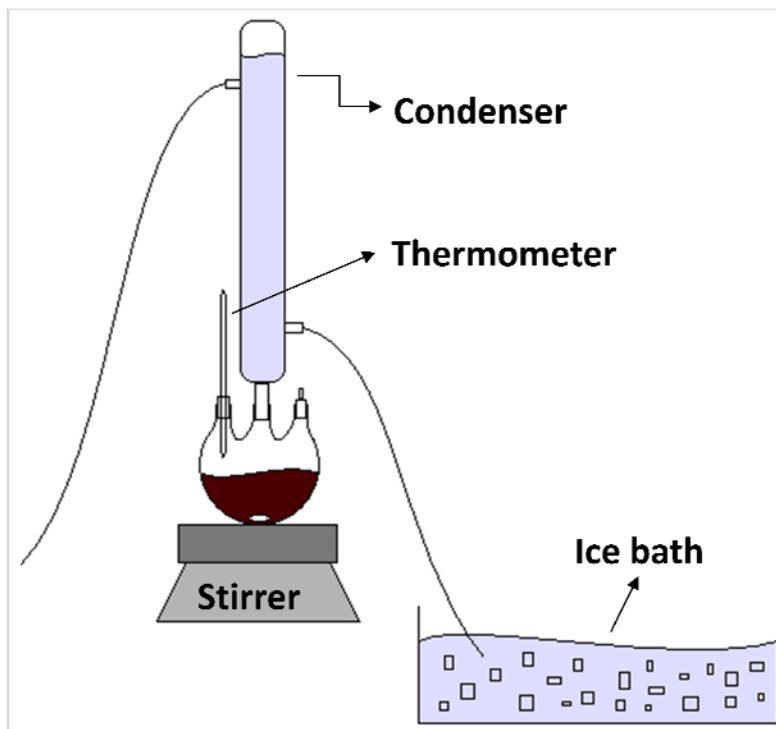


**Figure 5. Schematic Diagram of the equipment for the sulfonation reaction**

### **4.3 Sulfonation**

Sulfonation is a reaction in which a polymer is chemically modified by adding sulfonic groups,  $\text{SO}_3\text{H}$ , into their structure. The sulfonation of the polymers was performed using the suggested procedure for the sulfonation of SIBS [3], but modified for our unsaturated L-SIS/B-SI polymers (see Figure 6). SIBS polymers are sulfonated in the para-position of the aromatic ring in the styrene block of the polymer [3] as shown in Figure 7.

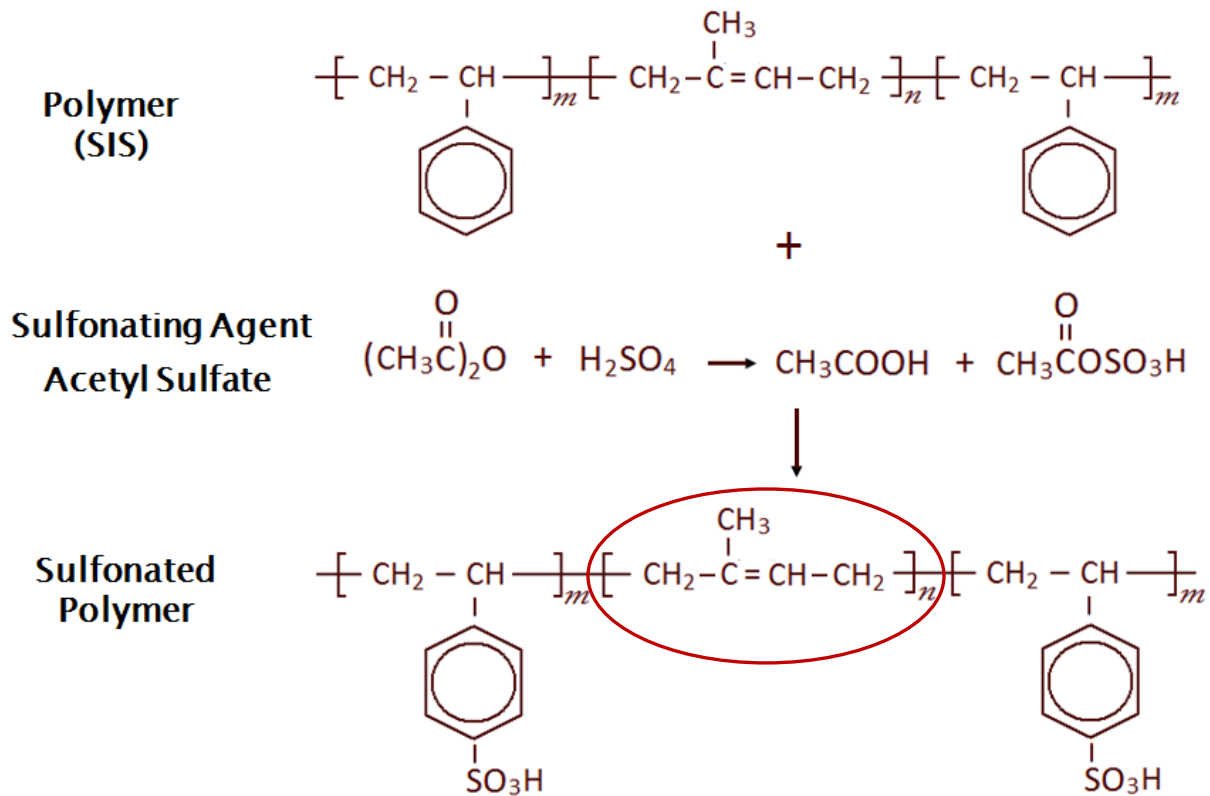


Figure 6. Sulfonation Reaction for the SIS/SI polymers

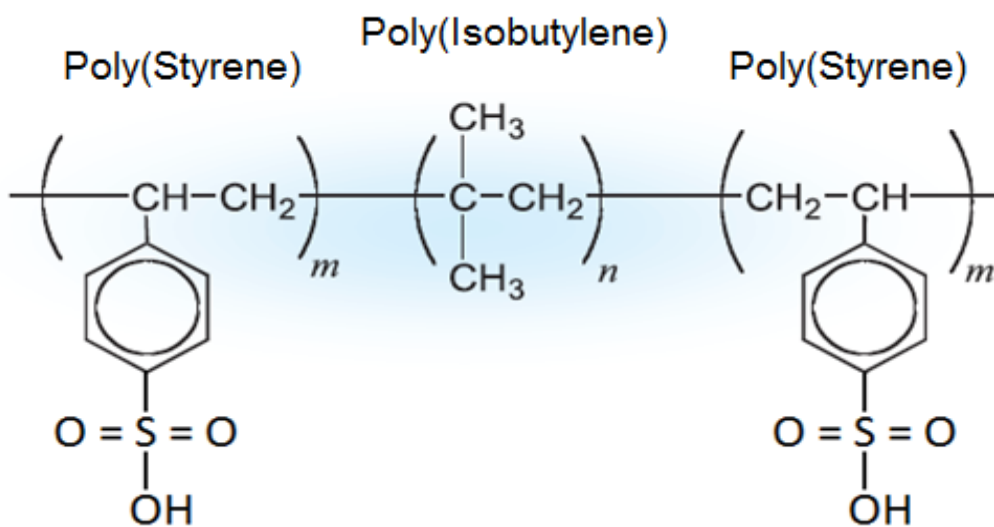
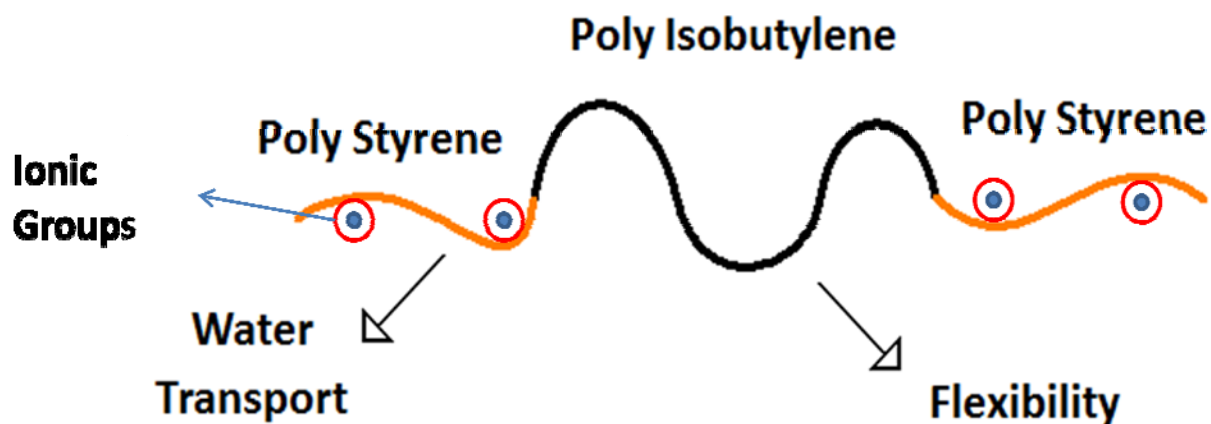


Figure 7. SIBS Chemical Structure with Sulfonic Groups

L-SIS/B-SI polymers have multiple sulfonated sites due to the additional  $\pi$  bonds from the PI block. The sulfonation level of the polymer was controlled with the stoichiometric amount of the sulfonating agent (acetyl sulfate). Additional methylene chloride (solvent) was also used to avoid evaporation caused by the exothermic sulfonation reaction. Figures 8 & 9 show the SIBS polymer chemical modifications in the ionic groups and the morphologies obtained after sulfonation. The phase morphology assumed by a given A-B-A triblock copolymer is dependent primarily on the relative volume fraction of the two constituent blocks. A block copolymer containing a low volume fraction of glassy end blocks will produce a morphology in which the glassy domains exist in isolated spheres throughout the rubbery matrix. As the volume fraction of glassy block is increased proportionally to the sulfonation level, the spherical domains become cylindrical and then lamellar [37].



**Figure 8. Chemical Modification of PS Blocks in SIBS Polymer**

**Figure 9. Chemical Morphologies after sulfonation**

#### **4.4 Blends**

Poly(isoprene) (PI), also known as natural rubber, is an elastomer. After stretching, elastomers have the ability to return back to its original size and shape due to entropic effects among the polymer chain (see Figure 10).

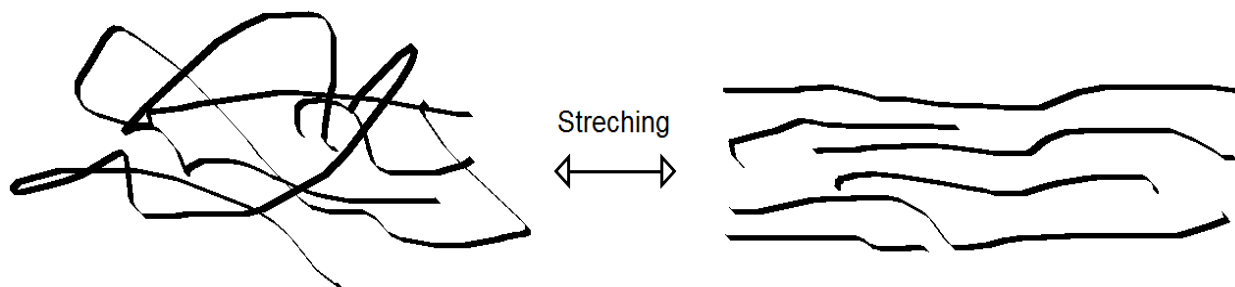


**Figure 10. Polymers Elastomeric Properties**

Elastomeric properties of the unsulfonated L-SIS/B-SI polymers changed after sulfonation. The PI block also reacts with the sulfonic groups creating a brittle membrane. The membrane has a phase segregation, in which the polymer chains can line up and pack together into extremely ordered arrangements, like crystals, minimizing the elastomeric properties (see Figure 11).



**Figure 11. Crystals Ordered Arrangements for polymers**

Polymer mixtures of sulfonated with unsulfonated polymers were prepared to recover the elastomeric properties. Blends preparation consist of mixing sulfonated L-SIS polymer with unsulfonated L-SIS/B-SI polymers in different weight percents or proportions. Linear/branched blends were prepared using L-SIS with 37% of sulfonation and mixed in 25/75 and 50/50 wt % relations with both linear and branched unsulfonated polymers. Blends of sulfonated branched polymers with 63% of sulfonation were also prepared but elastomeric properties were not

recovered due to the higher level of sulfonation. Experiments were conducted using only blends of sulfonated L-SIS polymer because there are the ones with the most consistent homogeneity and the elastomeric properties were recovered.

## 4.5 Membrane Casting

Sulfonated L-SIS/B-SI polymers and blends were dissolved in a mixed solution of toluene/hexanol (85/15) (w/w) with a concentration of 5% (w/v) and casted in open Teflon<sup>®</sup> Petri dishes using solvent casting at room temperature. Unsulfonated L-SIS/B-SI polymers were dissolved and casted using toluene or methylene chloride as solvents. Casted membranes were placed in a vacuum oven at 65°C to remove any residual solvent. Solvents have various chemical and physical properties that not only induce different interactions with polymer chains, also result in different phase inversion processes during the fabrication. Therefore, membranes prepared by different solvents may have different morphologies and performance [38]. For convenience, sulfonated membranes were labeled L-SIS-XX and B-SI-XX for linear and branched configuration, respectively, with XX corresponding to their respective sulfonation percent. The sulfonation mole percent was obtained after performing elemental analysis (EA). The mole percent sulfonation was based on the available sites for sulfonation from PS only. Linear blends were labeled M-LL-SIS-XX, indicating a blend mixture of unsulfonated L-SIS polymer and sulfonated L-SIS polymer followed by XX, which is the sulfonation mole percent obtained after elemental analysis. Branched blends were labeled M-BL-SIS-30-XX, representing a mixture of unsulfonated B-SI polymer with sulfonated L-SIS polymer followed by the % sulfonation after elemental analysis (EA).

## **4.6 Cation Substituted Cross-linked Membranes**

Counter-ion substitution was performed to increase the selectivity of the sulfonated membranes. Cations easily attach to the sulfonic groups due to the chemical deficiency of ions in the electron shell of the polymer chain. Salt solutions with  $\text{Ca}^{+2}$ ,  $\text{Ba}^{+2}$  and  $\text{Mg}^{+2}$  cations were used to analyze different effects in the membranes. The membranes were cross-linked by immersing them in a 1.0M solution of magnesium chloride ( $\text{MgCl}_2$ ), calcium chloride ( $\text{CaCl}_2$ ) or barium chloride ( $\text{BaCl}_2$ ) for 24 hours. Then, they were washed with deionized water and dried in an oven at approximately  $60^\circ\text{C}$  [39] for several days.

## **4.7 Characterization Techniques**

### **4.7.1 Elemental Analysis (EA)**

Sulfonation level of the membranes was obtained from the elemental analysis conducted by Atlantic Microlab, Inc. in Norcross, Georgia. Elemental analysis is a process where a sample of some material is analyzed for its elemental composition. Elemental analysis can be qualitative, determining what elements are present in the sample, and it can be quantitative, determining the specific amount (weight or mole percent) of an element in a compound. Functionalized membrane samples (1 – 3 mg) were analyzed for carbon, hydrogen and sulfur weight percents. Oxygen combustion under pressure is used for the sample preparation and the elemental analysis was performed using ion chromatography and inductively coupled plasma optical emission spectroscopy. Additional stoichiometric calculations were performed to obtain the final percent of sulfonation of all the membranes and linear/branched blends.

#### **4.7.2 Thermogravimetric Analysis (TGA)**

Thermogravimetry (TGA) is a technique that measures the change in weight of a sample as it is heated, cooled or held at constant temperature. Its main use is to characterize materials with regard to their composition. Application areas include plastics, elastomers and thermosets, mineral compounds and ceramics as well as a wide range of analyses in the chemical and pharmaceutical industries. The TGA is an exceptionally versatile tool for the characterization of physical and chemical material properties under precisely controlled atmospheric conditions. It yields valuable information for research, development and quality control in numerous fields such as plastics, minerals, pharmaceuticals and foodstuffs. TGA is useful to determine adsorption and desorption of gases, quantitative content analysis (moisture, fillers or polymer content), sublimation, evaporation and vaporization, identification of decomposition products, oxidation and thermal stability.

A Mettler Toledo TGA/SDTA 851E was used to study the thermal stability of the polymers, the degradation temperature behaviors of the membranes and the absorbed moisture or volatiles content of materials. TGA is performed to determine the amount of weight changes as function of increasing temperature in an atmosphere of nitrogen. A membrane sample weighting approximately 5 - 6 mg was used for each experiment. Degradation temperatures were determined by heating the polymer samples in the nitrogen environment to 650°C at 10°C/min and observing regions of significant weight or mass loss [39].

### 4.7.3 Water Swelling

Water swelling, also known as solubility, is a measure of how much moisture is absorbed by the membrane during a period of time. The measurements of water-swelling ratio were performed using a membrane sample between 20 – 40 mg, by the immersion/gain method. The sample was dried for 24 hours at 70 °C in an oven, and its original weight was recorded. Then, it was immersed in an excess amount of HPLC water solution (5 mL) at room temperature (23 °C). The effect of temperature on water-swelling ratio was not considered for this experiment. The weight of wet membranes was determined after different times until swelling equilibrium was reached [3]. Each reported result represents the average of three repetitions.

### 4.7.4 Permeability

#### 4.7.4.1 Theory

Fick's first law is used in steady state diffusion, when the concentration within the diffusion volume does not change with respect to time. Diffusion occurs in response to a concentration gradient expressed as the change in concentration due to a change in position and can be expressed by the Fick's first law of diffusion:

$$J_A = -D_{AB} \frac{dC_A}{dx_A}$$

in which the flux  $J_A$  [ $\text{mol cm}^{-2} \text{s}^{-1}$ ] is proportional to the diffusivity  $D_{AB}$  [ $\text{cm}^2/\text{s}$ ] and the negative gradient of concentration,  $\frac{dC_A}{dx_A}$  [ $\text{mol cm}^{-4}$ ]. The diffusion flux,  $J_A$ , measures the amount of

substance that will flow through a area during a period of time and for vapor transport studies is equal to the vapor transfer rate (VTR).

The vapor transfer rate (VTR) is a transfer rate measure of a permeant through a membrane in the vapor phase. This rate does not take into consideration the membrane thickness but relates the permeant weight with the time and the area of exposure by the following equation:

$$VTR = \frac{W}{t * A}$$

where  $W$  is the permeant weight (g),  $t$  is the time (hr) and  $A$  is the cross-sectional area ( $m^2$ ). The vapor transfer rate was obtained from the slope of the linear regression of the steady state part of the weight loss data vs. time.

In order to obtain a better understanding in the vapor transfer studies it is necessary to calculate the effective permeability ( $P_{eff}$ ) of the membranes using the Fick's law:

$$P_{eff} = \frac{L * VTR}{\Delta C_i}$$

where  $L$  is the membrane thickness (m),  $VTR$  is the vapor transfer rate ( $g/m^2$  hr) and  $\Delta C_i$  is the permeant concentration change during the experiment. The change in concentration can be calculated using the ideal gas equation obtaining the final equation

$$P_{eff} = \frac{L * VTR}{\frac{MW_i}{RT} (P_{i_1} - P_{i_2})}$$

where  $P_{i_1}$  is the partial pressure of the permeant inside the vial (mmHg),  $P_{i_2}$  is the partial pressure of the permeant outside the vial (mmHg),  $R$  is the gas constant ( $\text{m}^3 \cdot \text{mmHg} / \text{mol} \cdot \text{K}$ ),  $T$  is the experiment temperature and  $MW_i$  is the permeant molecular weight (g/mol). For this experiment, there is 100% permeant saturation because  $P_{i_1} = P_i^{vap}$  in the challenge side (inside the vial) and 0% of permeant outside the vial because  $N_2$  takes all the permeant away and  $P_{N_2} \gg P_{i_2}$ , simplifying the equation to

$$P_{eff} = \frac{L * VTR}{\left( P_i^{vap} \frac{MW_i}{RT} \right)}$$

This equation considers the membrane thickness and is a more accurately measure to compare different types of materials.

#### 4.7.4.2 Permeability Experiments

Permeability experiments were conducted based on vapor transport studies using an oven at 35°C with an inert atmosphere of nitrogen, an analytical balance (precision = 0.0001g) to measure weight loss, and 20 mL vials of open top caps with a 6mm hole cut in the center of the Teflon septa, as shown in Figure 12. The membrane thickness was measured prior to the experiment with a vernier caliper.

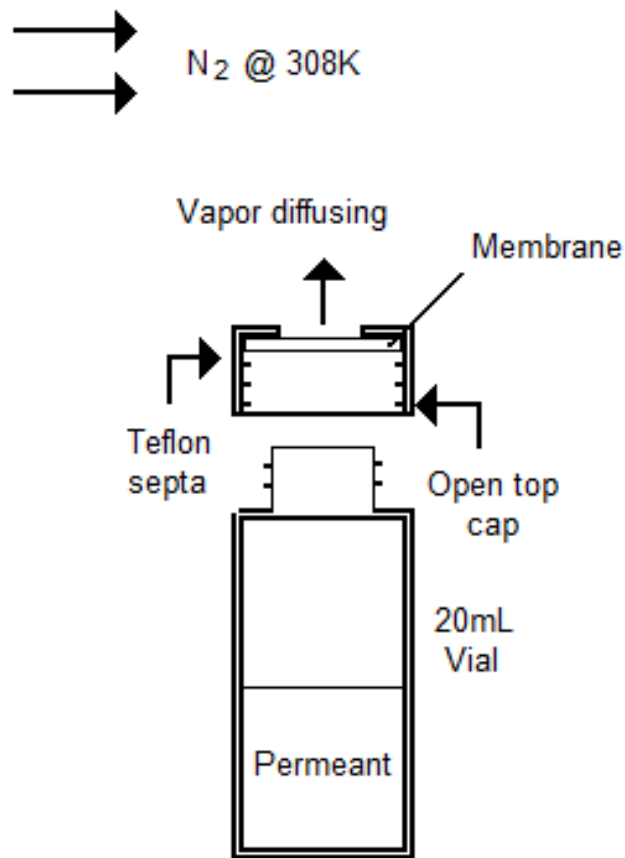


**Figure 12. Schematic Diagram for Vapor Permeation**

Vials were filled with 5 mL of DMMP or 5 mL of water depending on the permeant analyzed and placed into the oven. Weight measurements were performed for a period of time. DMMP, with chemical formula  $\text{CH}_3\text{PO}(\text{OCH}_3)_2$ , was selected as a simulant for the chemical toxin Sarin (GB) (nerve gas), due to its similarity in chemical structure, physical properties and volatility (see Figure 13). Nerve agents are organic phosphorus compounds, i.e. esters of phosphonic or phosphoric acid as are some insecticides, flame retardants, plasticizers, softeners, emulsifiers and lubricating oil additives [40].

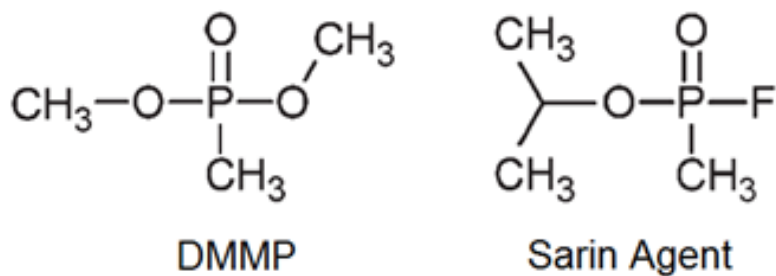


**Figure 13. Chemical Structures of DMMP and Sarin toxic Agent**

#### 4.7.5 FT-IR Spectroscopy

Infrared spectroscopy [41] is an important and universal technique for the chemical analysis to identify the components or measuring the concentration of molecules in a sample. The infrared absorption process occurs when molecules get excited to a higher energy state when they absorb infrared radiation and is related to the stretching, contracting and bending vibrational frequencies of the bonds in most of the covalent molecules. The infrared spectra obtained by this technique in the spectrometers or spectrophotometers are plots of measured infrared intensity versus wavenumber and the peak intensities are proportional to concentration. In the infrared spectrometer it is possible to analyze solids, liquids, powders and polymers among others. FT-IR spectroscopy was used to detect chemical functional groups of organic compounds and to confirm identities with the peak positions and intensities. Infrared spectra were collected in a Thermo Nicolet IR-300. A special attenuated total reflectance (ATR) attachment was used for solid IR spectra. 64 scans were taken with a resolution of  $4\text{ cm}^{-1}$  and the spectra were obtained from  $4000$  to  $400\text{ cm}^{-1}$ .

#### 4.7.5.1 Stretching and Bending Vibrations

Stretching and bending are the two simplest types of vibrational motion frequencies. The  $\text{SO}_2$  vibrational frequencies are presented in Figures 14 & 15. In general, asymmetric stretching vibrations occur at higher frequencies than symmetric stretching vibrations and all stretching vibrations occur at higher frequencies than bending vibrations. Molecules with two identical atoms have two modes of stretching: symmetric and asymmetric [42].

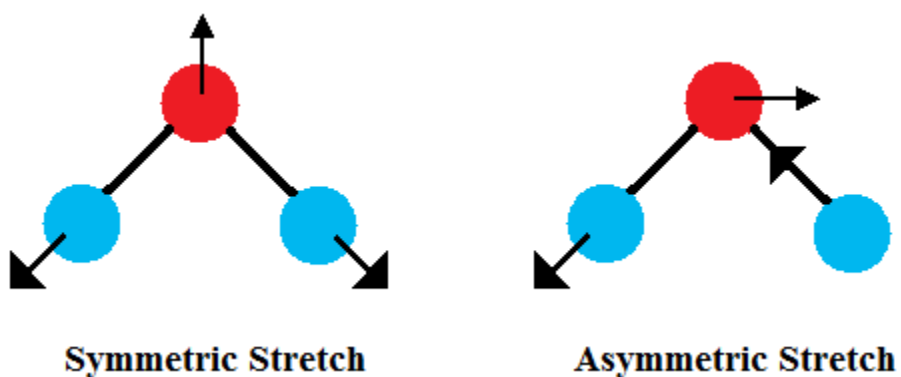


**Figure 14. Symmetric and asymmetric stretching vibrations for the  $\text{SO}_2$  molecule**

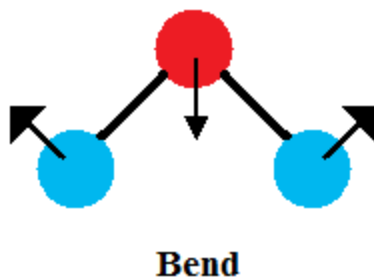


**Figure 15. Bending vibration for the  $\text{SO}_2$  molecule**

Herzberg et al. [43] described the valence force model as a way to analyze the vibrations and determine the force constants of the stretches and bends. In this model, it is assumed that there is large restoring force along the chemical bond when the equilibrium position of this molecule is disturbed. This same type of restoring forces is assumed to affect any perturbations in the angle between two adjacent bonds. It is possible to use this valence force model to describe the force constants of the SO<sub>2</sub> molecule, using the potential energy for a better behavior understanding.

#### 4.7.5.2 Infrared Spectroscopy of Organic Sulfur Compounds

Sulfur is most commonly found bonded to one, two, three, or more oxygen atoms forming different functional groups. Also, sulfur can form bonds with hydrogen, carbon, or even with other sulfur atoms. Sulfur – oxygen bonds have high and intense infrared peaks because of the molecular dipole moment. This dipole-dipole moment occurs with polar molecules in which there exists an attraction between a pole of a molecule and the opposite pole of other molecule. Sulfur – sulfur, sulfur – hydrogen and carbon – sulfur bonds have low and weak infrared peaks because of the small dipole moment making the infrared spectroscopy detection difficult [41].

##### a. Thiols or Mercaptans

Thiol functional group contains sulfur – hydrogen (S – H) and carbon – sulfur (C – S) single bonds. Thiol bands in infrared spectrums are weak in intensity due to the dipole moment. In the liquid phase, this functional group is found in a wavenumber between 2590 and 2560 cm<sup>-1</sup>. For solids, it is more complicated and not easy to view.

#### b. Sulfoxides and Sulfites

Sulfoxides are molecules that contain one sulfur – oxygen double bond (S=O) and two carbon – sulfur single bonds (C – S). The S=O stretch is the most important infrared band of this group appearing from 1070 to 1030  $\text{cm}^{-1}$ . Sulfites contain one sulfur – oxygen double bond (S=O) and two sulfur – oxygen single bonds (S – O). This functional group has a strong S=O vibration and appears in the range of 1240 to 1180  $\text{cm}^{-1}$  of the infrared spectrum. Wavenumbers of S=O stretch increases as more oxygen are added to the sulfur atom.

#### c. Sulfones, Sulfonates and Sulfates

All these functional groups have two sulfur – oxygen double bonds (O=S=O or  $\text{SO}_2$ ) in common, but differ in the number of S – O bonds containing zero for the sulfone group, one for the sulfonate group and two for the sulfate group, specifically. The  $\text{SO}_2$  group has symmetric and asymmetric stretching vibrations due to its linearity between 1450 and 1150  $\text{cm}^{-1}$ . For sulfones the symmetric and asymmetric  $\text{SO}_2$  stretches appear in the range of 1340 to 1310  $\text{cm}^{-1}$  and 1165 to 1135  $\text{cm}^{-1}$ , respectively. In sulfonate groups these stretches bands occur between 1430 to 1330  $\text{cm}^{-1}$  and 1200 to 1150  $\text{cm}^{-1}$ .  $\text{SO}_2$  stretches in sulfates appear from 1450 to 1350  $\text{cm}^{-1}$  and 1230 to 1150  $\text{cm}^{-1}$ .

### 4.7.6 Small Angle X-Ray Scattering (SAXS)

The Small Angle X-Ray Scattering (SAXS) was useful to obtain information about the structure and morphology of the nanochannels in the membranes. SAXS experiments were conducted using a one dimension SAXSess mc<sup>2</sup> in the Chemical Engineering Department of the University of Washington, Seattle and a SAXSquan<sup>TM</sup>-Software was used for the data analysis.

SAXS mc<sup>2</sup> is the better equipment for the nanostructure analysis using small-angle X-ray scattering (SAXS).

SAXS provides information on the overall size and shape of nanosized particles scattering toward small angles and is used for the analysis of nanostructure ranging from 1 to 150 nm. Specifically, SAXS determines internal structure, shape, size, crystallinity, and porosity. This makes it a universal tool for investigating nanostructures in different materials, including proteins, foods, pharmaceuticals, polymers, nanoparticles, and catalysts. SAXS is an accurate, economical, and non-destructive method for the characterization of nanomaterials. When X-rays penetrate a nanostructured material they are scattered on the interfaces of the nanostructures at certain scattering angle. The resulting scattering pattern is specific to the structure and is used to characterize the nanomaterial. A typical SAXS system comprises an X-ray source, optics, a collimation system, the sample stage, a beam stop and a detector.

#### 4.7.6.1 SAXS Instrument Resolution

SAXS experiments were performed in order to reveal structures owing to its close relationship to microscopy. In any optical experiment objects with diameter of size  $D$  can be determined only in a resolution-limited range between  $D_{min}$  and  $D_{max}$ . In SAXS these limits are defined by the wavelength of the X-ray radiation and by the aperture of lens, i.e., the range of scattering angles between which the scattering pattern is sampled. Using the sampling theorem of the Fourier transformation the scattering profile, which is measured between  $q_{min}$  and  $q_{max}$ , can be used to resolve particle features only between  $D_{min}$  and  $D_{max}$ , where  $D_{min} = \frac{\pi}{q_{max}}$  and  $D_{max} = \frac{\pi}{q_{min}}$ , where  $q$  is the scattering vector and  $D$  is the resolution diameter of each nanostructure.

In SAXS technology the challenge is to reach a small  $q_{min}$  without disturbance. The quality of SAXS instruments are usually specified in terms of  $q_{min}$  or  $D_{max}$  with a resolution of  $D_{max} = 30 - 50\text{nm}$ . Commonly, the largest distance is specified by  $d_{max} = \frac{2\pi}{q_{min}}$ , where  $d_{max}$  is the maximum lattice spacing of a crystal plane and  $q_{min}$  is the minimum length of the scattering vector or the momentum transfer. The lattice distance is two times larger than the resolution limit. That is the reason for the discrepancy factor of 2 is between  $d_{max}$  and  $D_{max}$  [44].

#### **4.7.7 Scanning Electron Microscope (SEM)**

The scanning electron microscope (SEM) is a microscope that uses electrons to produce images of high resolution. SEM provides a good representation of the three-dimensional sample and is designed for the study of solid surfaces. The samples must be dry, non-living, and coated with some material to make them electrically conducting. For this experiment samples were coated with a layer of gold and then analyzed in the SEM at different magnitudes of resolution.

## 5 Results and Discussions

### 5.1 Sulfonation Analysis

Sulfonation levels may vary depending on the reaction conditions (time and the sulfonating agent/polymer relation). Table 2 shows all the sulfonation levels obtained for the linear and branched membranes at different reaction conditions. High sulfonation levels of 93.2% and 106.10% were obtained for linear SIS and branched SI polymers, respectively. Values over 100% in branched membranes indicate additional sulfonation sites to the para position of the styrene ring; both L-SIS and B-SI showed sulfonation in the  $\pi$  electrons of PI as well. Table 3 shows sulfonation level results for blends. Blends values were lower because they included unsulfonated L-SIS/B-SI polymers to preserve the elastomeric behavior of the membranes.

Membrane Name	Sulfonation Level (%)	Reaction Time (hr)	Relation (Acetyl Sulfate:Polymer)
L-SIS-7.0	6.99	½	2:1
L-SIS-8.2	8.23	1	2:1
L-SIS-8.7	8.71	1	2:1
L-SIS-17.2	17.24	2	2:1
L-SIS-27.5	27.50	5	2:1
L-SIS-37.8	37.82	19	2:1
L-SIS-93.2	93.21	19	4:1
B-SI-14.1	14.09	½	2:1
B-SI-61.9	61.92	1	2:1
B-SI-63.0	63.03	19	2:1
B-SI-106.1	106.10	19	4:1

**Table 2. SIS/SI Sulfonation levels**

Blend Name	Sulfonation Level (%)
M-LL-SIS-9.7	9.67
M-LL-SIS-14.3	14.35
M-BL-SIS-12.6	12.57
M-BL-SIS-23.3	23.27
M-LB-SI-27.0	26.99
M-LB-SI-57.1	57.07
M-BB-SI-18.8	18.80
M-BB-SI-53.8	53.81

**Table 3. Blends Sulfonation Levels**

## 5.2 Degradation Temperatures

Un sulfonated L-SIS and B-SI only show two degradation temperatures, the first one is due to the PI decomposition and the second one to the PS decomposition (see Figures 16 & 17). The patterns as well as the degradation temperatures of both L-SIS and B-SI are the same. Sulfonated SIS and SI have four weight loss stages with four degradation temperatures, as shown in Figures 18 & 19. The first and second weight loss stages in the 50-200°C range are attributed to the atmospheric moisture or water absorbed by the hygroscopic sulfonated L-SIS polymer. The third weight loss stage occurs at 250-400°C and is attributed to the decomposition of the sulfonate groups in the polymer. The last weight loss stage in the 390-475°C range is due to the polymer backbone degradation. Un sulfonated linear SIS and branched SI have very similar thermal stability (PIB degrading at 378°C and PS degrading at 428°C). However, upon sulfonation their thermogravimetric behavior showed the disappearance of the mass at 378°C, and the appearance of an additional mass at 254°C (branched) and 270°C (linear) which could be

attributed to sulfonated PS. Sulfonation of the PI blocks created additional unique degradations at lower temperatures (178°C linear and 161°C branched), which were not observed in the unsulfonated polymers. Sulfonation process adds stability to the polymer increasing their degradation temperature by 8.4°C in L-SIS and 11.6°C in B-SI. Also, the sulfonated polymers only show one polymer degradation temperature instead of the individual PI and PS components as in the unsulfonated polymers. The degradation temperatures of sulfonated L-SIS and B-SI were different in all four regions indicative of morphological differences between the sulfonated linear vs. branched configurations. Table 4 shows the exact degradation temperatures for unsulfonated/sulfonated linear and branched polymers.

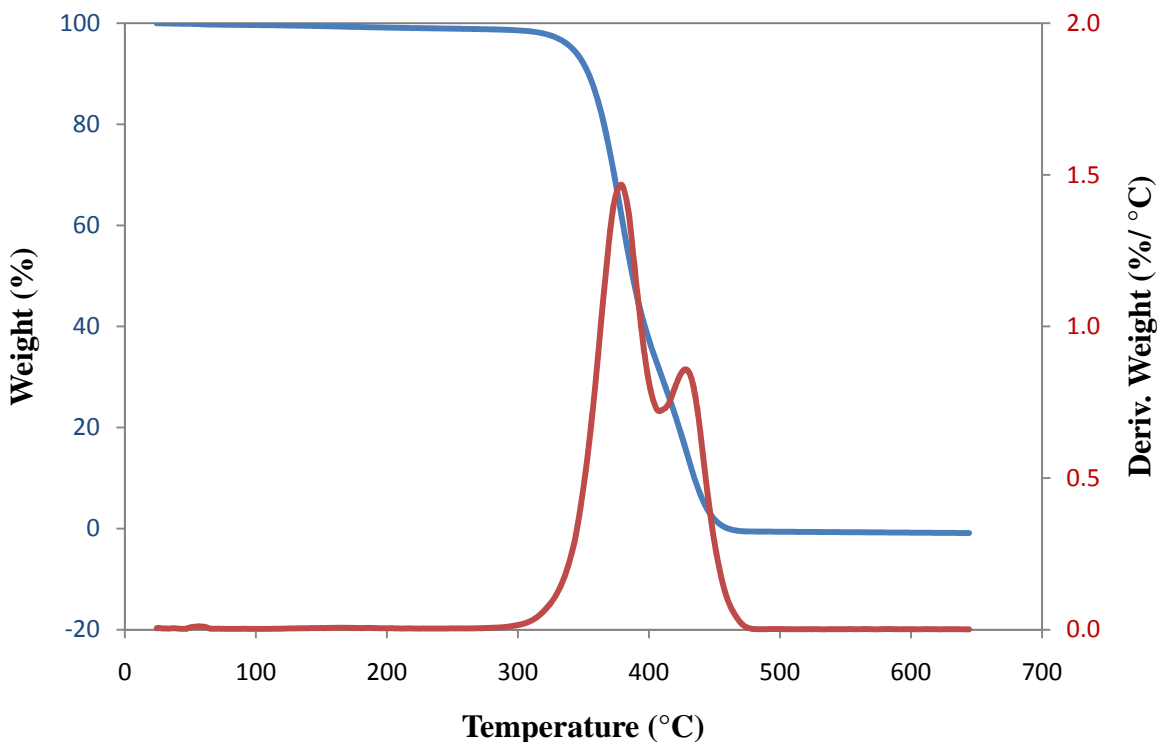


**Figure 16. Thermogravimetric Analysis (TGA) for L-SIS-0.0**

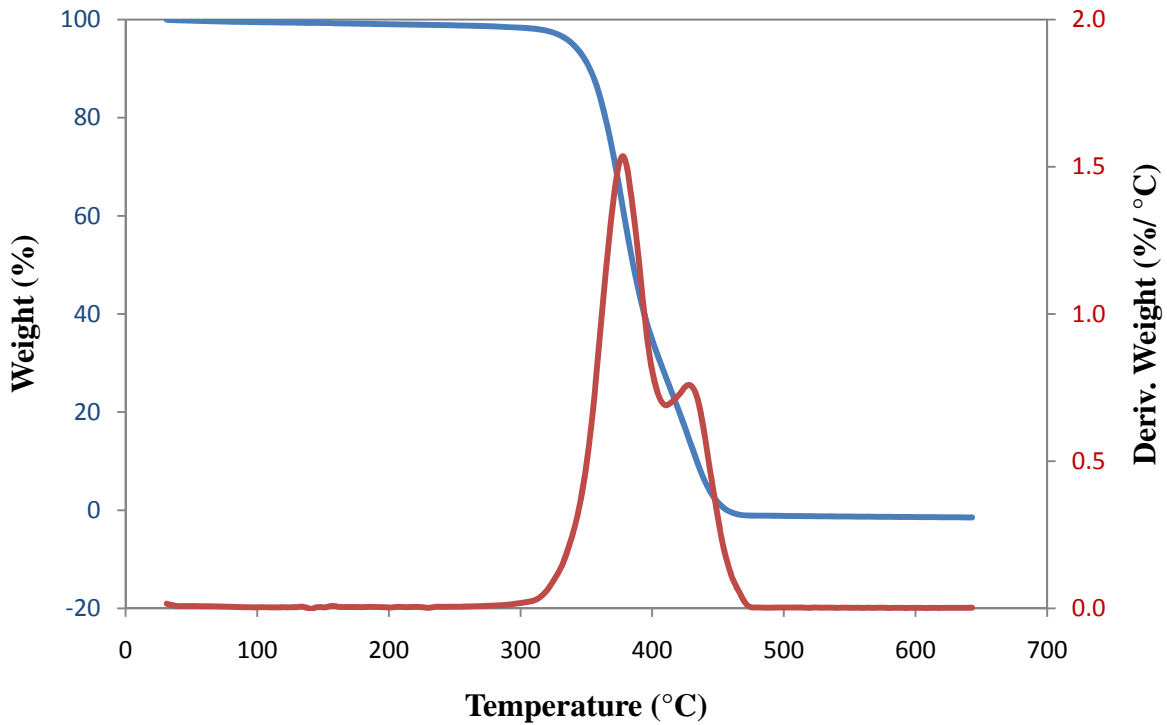


**Figure 17. Thermogravimetric Analysis (TGA) for B-SI-0.0**

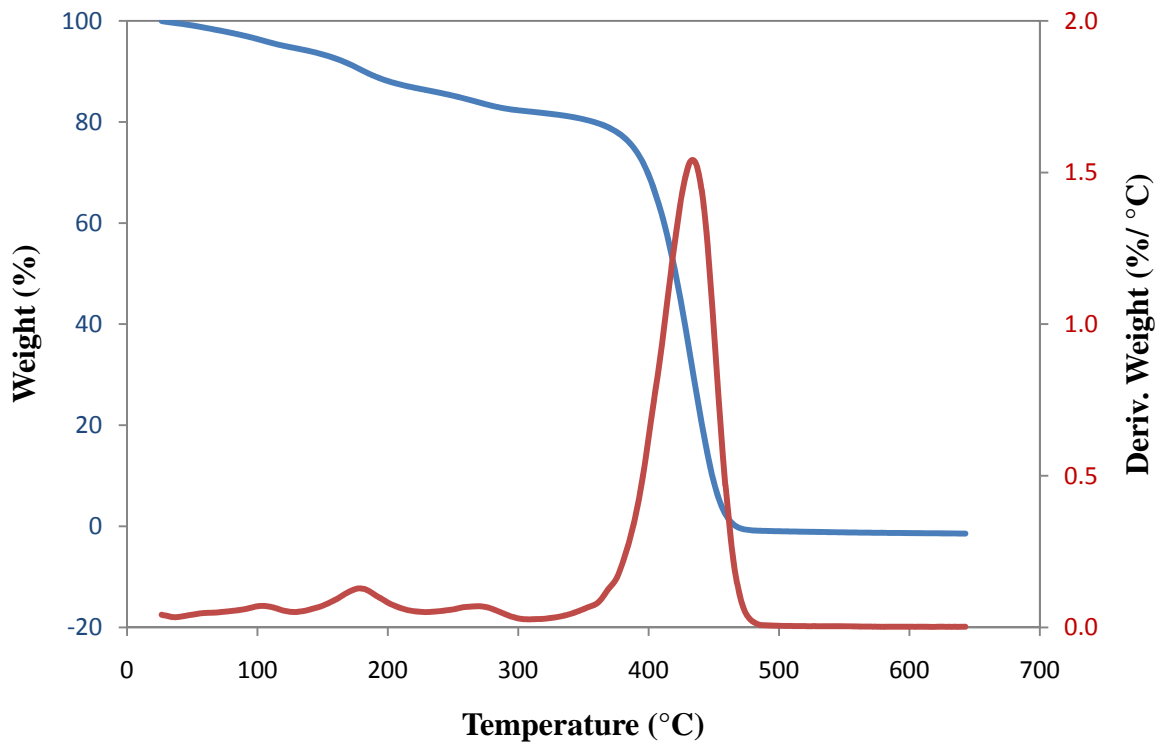


**Figure 18. Thermogravimetric Analysis (TGA) for L-SIS-37.8**

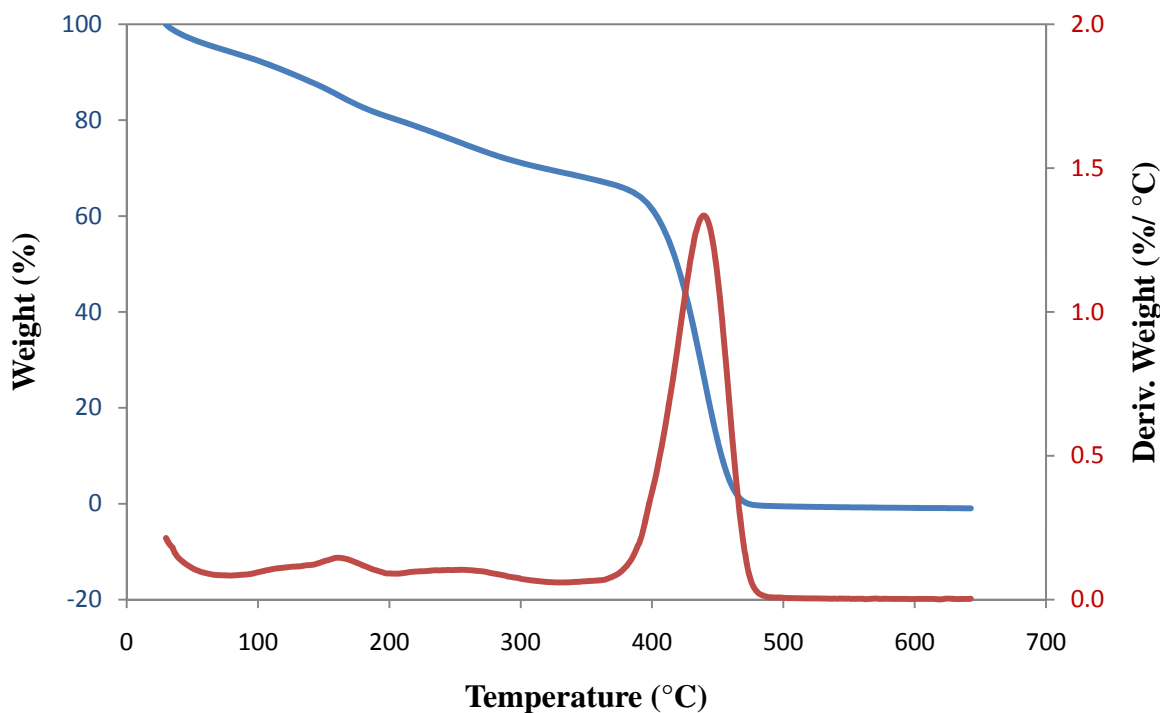


**Figure 19. Thermogravimetric Analysis (TGA) for B-SI-63.0**

Block Copolymer	1 <sup>st</sup> Tg (°C)	2 <sup>nd</sup> Tg (°C)	3 <sup>rd</sup> Tg (°C)	4 <sup>th</sup> Tg (°C)
L-SIS-0.0	-	-	378.7	427.9
L-SIS-37.8	103.7	178.4	269.9	436.3
B-SI-0.0	-	-	377.5	427.8
B-SI-63.0	127.4	161.0	254.3	439.4

**Table 4. Degradation Temperatures for sulfonated/unsulfonated linear/branched SIS**

### 5.2.1 Blends

TGA results for the blends are presented in Figures 20 – 23. Figures 20 & 21 represent blends of linear polymers with different percent (%) sulfonation. The first degradation

temperature occurs in the range of 300°C – 400°C for M-LL-SIS-9.7 and 320°C – 395°C for M-LL-SIS-14.3. The second degradation temperature is in the same region for both. Blends that incorporated branched polymers, also present similar behavior with one degradation temperature in the range of 300°C – 400°C, but differed in the second degradation region (Figures 22 & 23). Branched blends are more thermally stable than Linear blends. Similarities among linear and branched blends depend on weight percent relation of linear/branched blends and not in morphological differences. Low sulfonation levels are obtained for these linear/branched blends, and although no distinctive degradation was observed around 230 – 300°C, the decrease in weight below 300°C confirms the presence of sulfonic groups. Table 5 shows the exact degradation temperatures for linear and branched blends.

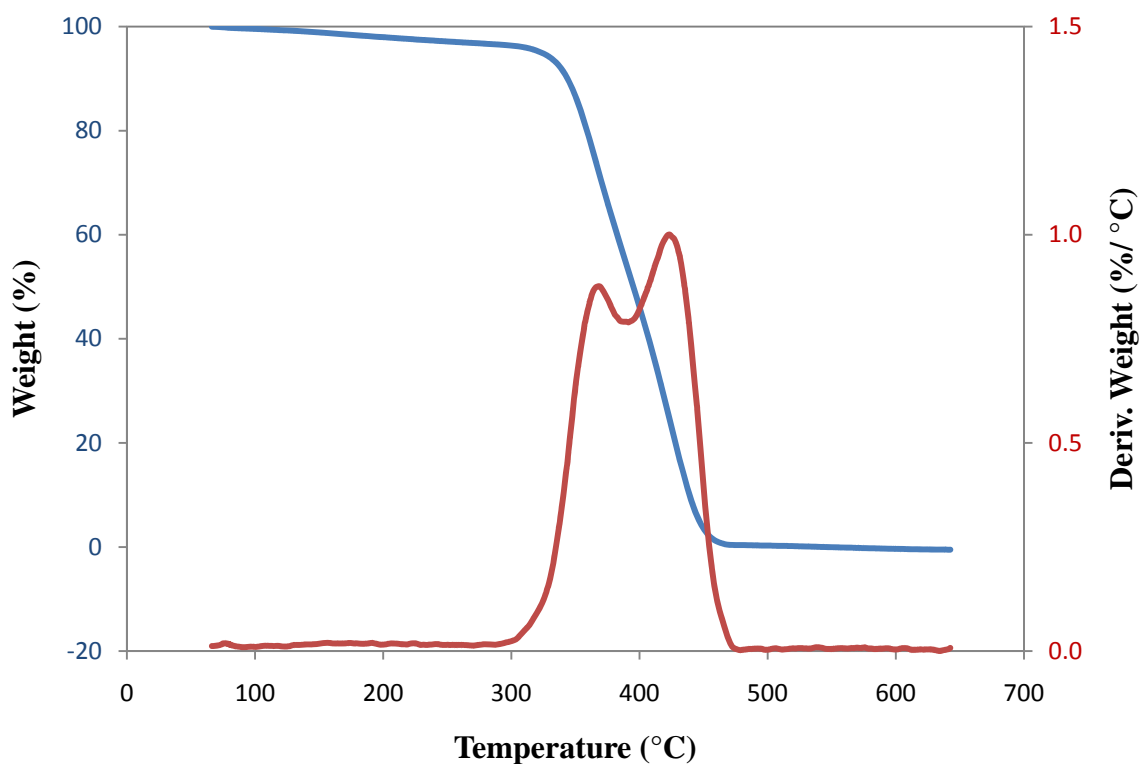


**Figure 20. Thermogravimetric Analysis (TGA) for M-LL-SIS-9.7**

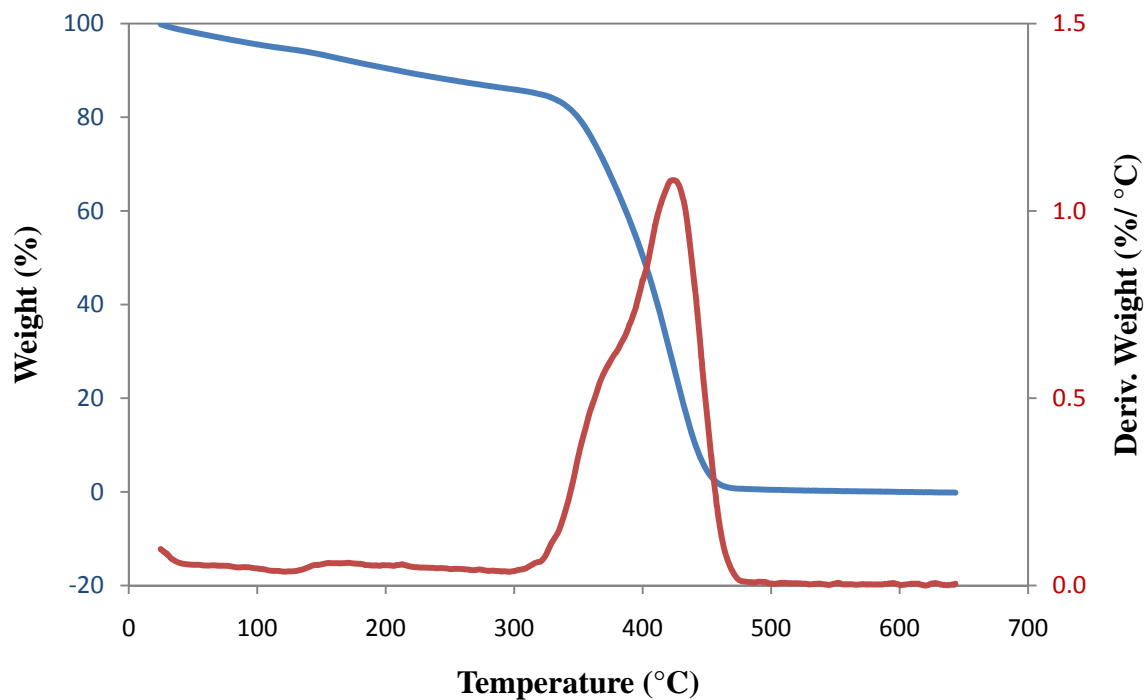


**Figure 21. Thermogravimetric Analysis (TGA) for M-LL-SIS-14.3**

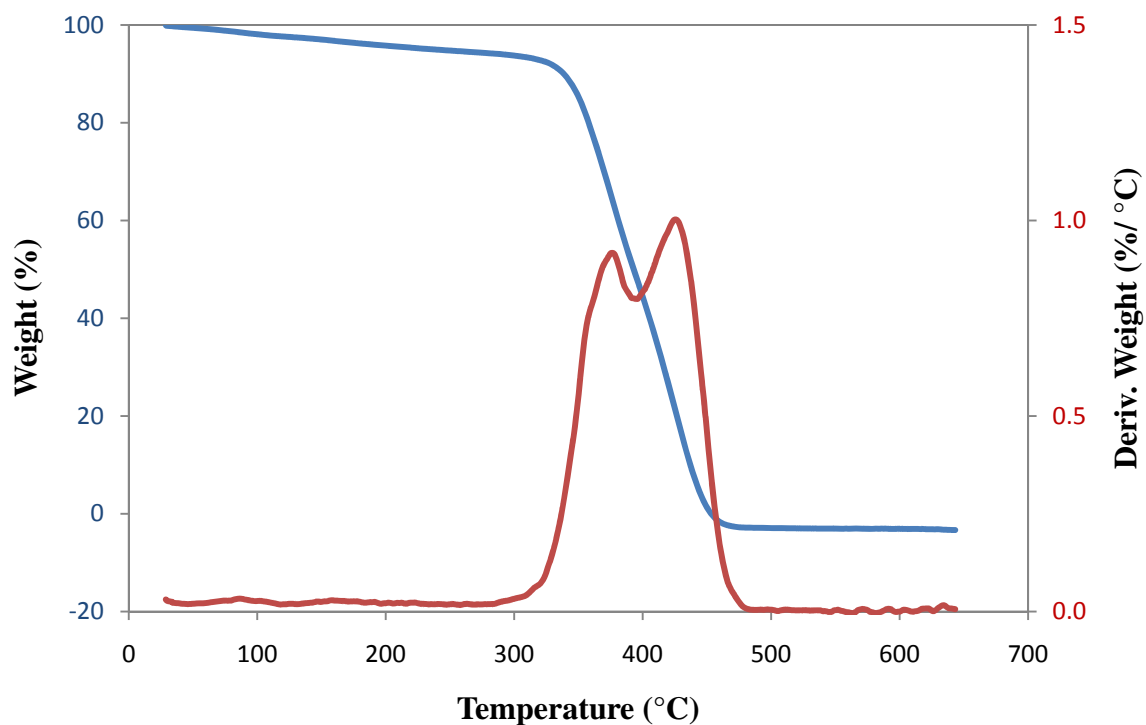


**Figure 22. Thermogravimetric Analysis (TGA) for M-BL-SIS-12.6**

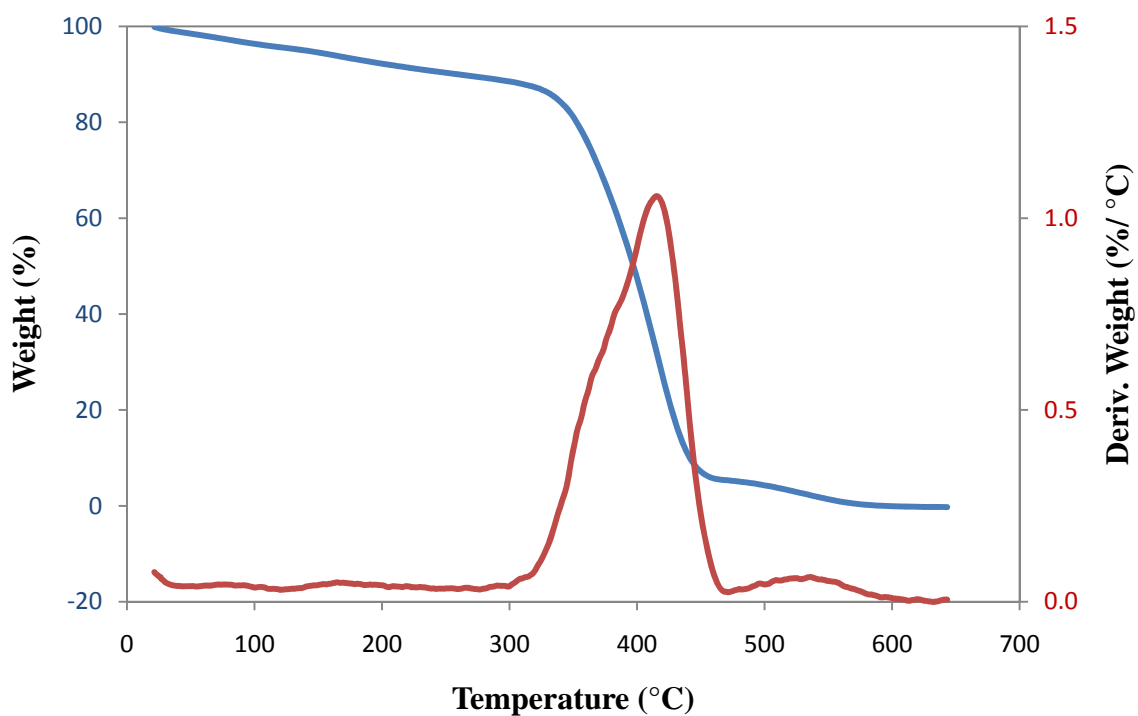


**Figure 23. Thermogravimetric Analysis (TGA) for M-BL-SIS-23.3**

<b>Block Copolymer</b>	<b>1<sup>st</sup> Tg (°C)</b>	<b>2<sup>nd</sup> Tg (°C)</b>	<b>3<sup>rd</sup> Tg (°C)</b>	<b>4<sup>th</sup> Tg (°C)</b>
M-LL-SIS-9.7	-	-	368.3	423.1
M-LL-SIS-14.3	-	-	-	423.6
M-BL-SIS-12.6	-	-	376.1	425.1
M-BL-SIS-23.3	-	-	-	450.3

**Table 5. Degradation Temperatures for linear and branched blends**

### 5.3 Water Swelling

Water swelling is related to the moisture absorbed by the sulfonic groups. At high sulfonation levels, higher water swellings are expected. Figures 24-28 show the results for water swelling experiments of the blends and the cation cross-linked membranes. Figure 24 compares linear vs. branched blends of different sulfonation levels. Significant differences are observed between linear and branched blends. Branched blends had higher water swelling and no significant differences were observed for different sulfonation mole percent. The largest amount of water swelling (up to approximately 22 wt%) was obtained for M-BL-SIS-23.3-Mg membrane (Figure 28).

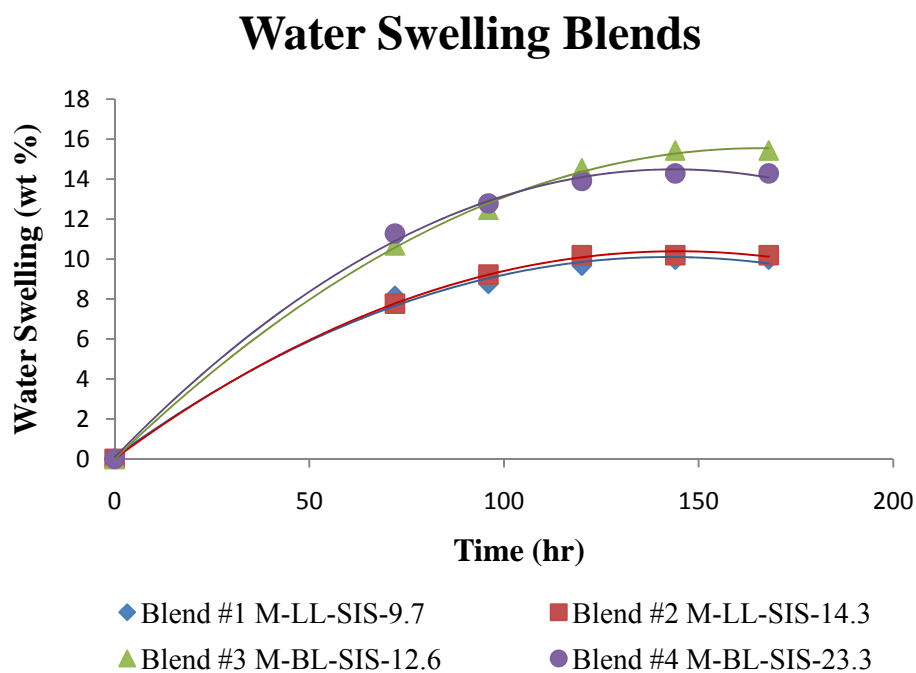


Figure 24. Linear vs. Branched effects on Water Swelling Studies

### Water Swelling M-LL-SIS-9.7 Blend

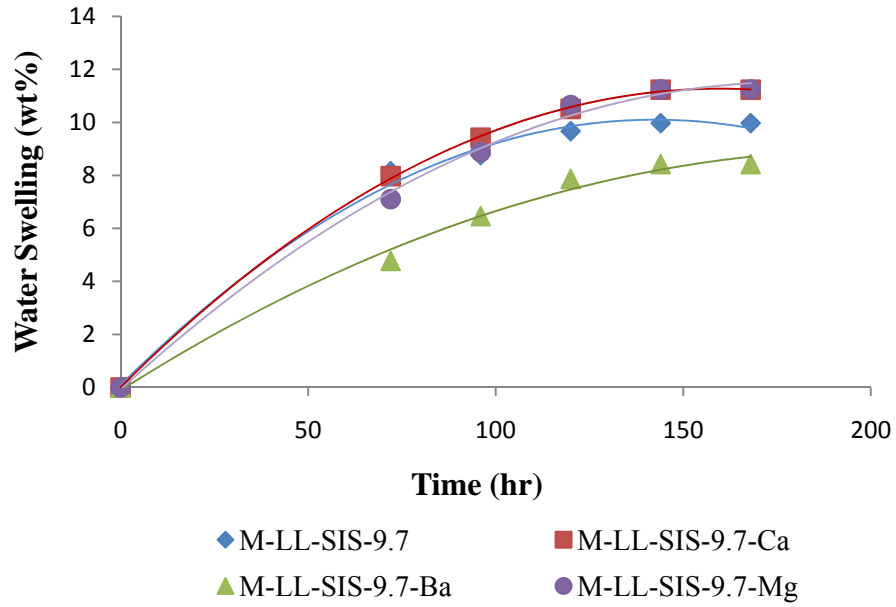


Figure 25. Cations Effect on Water Swelling Studies for M-BL-SIS-9.7 Blend

### Water Swelling M-LL-SIS-14.3 Blend

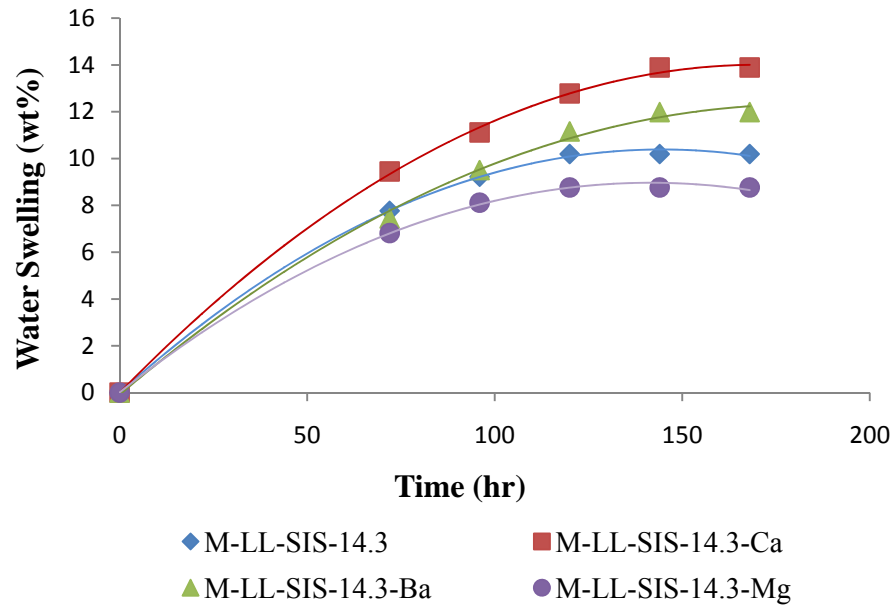


Figure 26. Cations Effect on Water Swelling Studies for M-BL-SIS-14.3 Blend

### Water Swelling M-BL-SIS-12.6 Blend

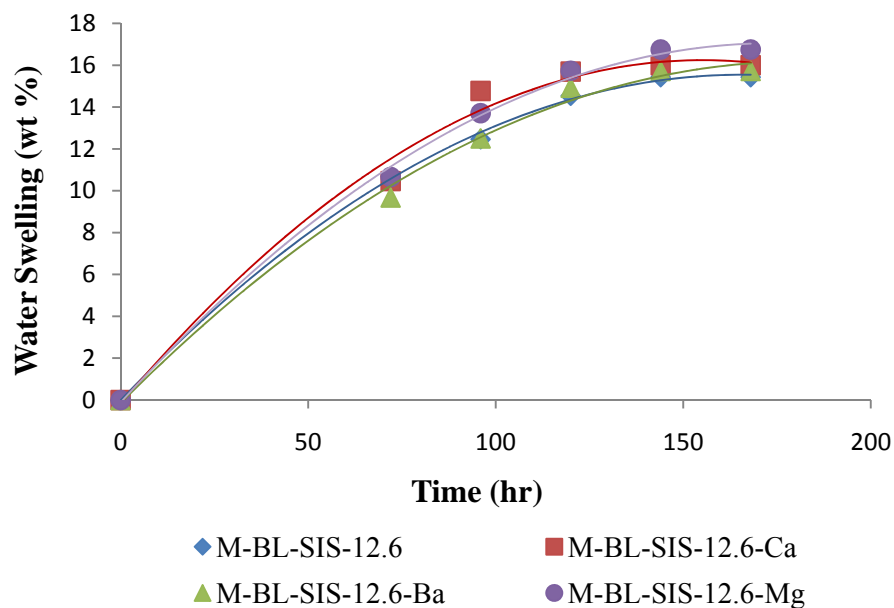


Figure 27. Cations Effect on Water Swelling Studies for M-BL-SIS-12.6 Blend

### Water Swelling M-BL-SIS-23.3 Blend

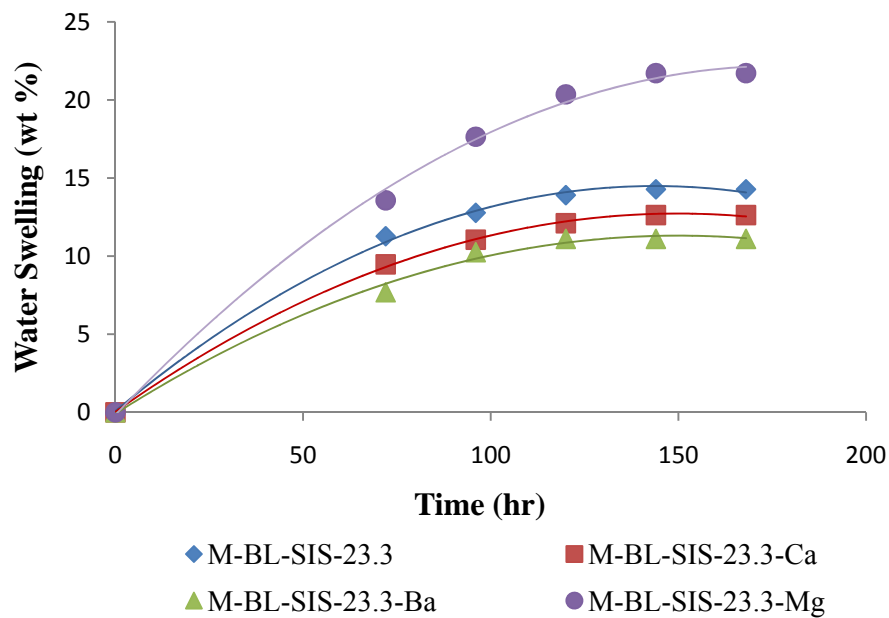


Figure 28. Cations Effect on Water Swelling Studies for M-BL-SIS-23.3 Blend

## 5.4 Permeability

### 5.4.1 Permeability Analysis

Vapor transfer studies are useful to select which type of membrane is more selective for chemical and biological protective clothing application. The goal is perform a material with a high breathability ( $\uparrow$  Water  $P_{\text{eff}}$ ) and good barrier properties against toxic agents ( $\downarrow$  DMMP  $P_{\text{eff}}$ ).

Breathability of the sulfonated/functionalized membranes was measured using water vapor transfer studies (Water VTR &  $P_{\text{eff}}$ ). Results show higher water transfer through M-LL-SIS-14.3 membrane, which means that linear blends with high sulfonation levels are the most promising for breathability purposes (Figures 29 & 30).

The effect of toxic agents against the membranes was analyzed using DMMP transfer studies (DMMP VTR &  $P_{\text{eff}}$ ). DMMP vapor transfer showed lower permeabilities in branched blends (Figures 31 and 32).

In general, DMMP vapor transfer rates and effective permeabilities are higher than the vapor transfer rates and effective permeabilities for water through the membranes.

## Water Vapor Transfer Rate (VTR)

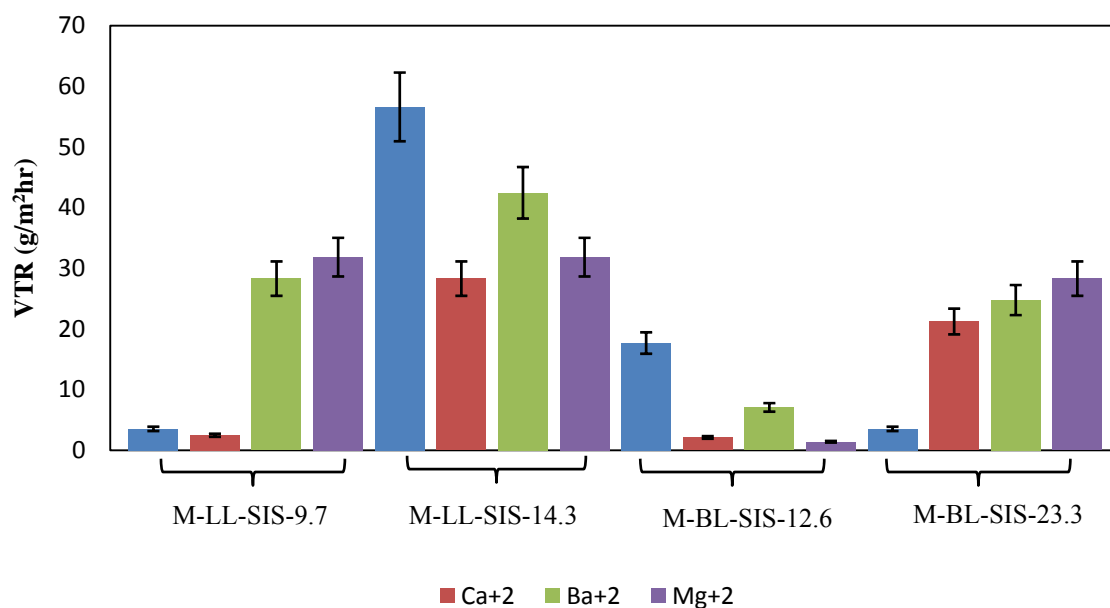


Figure 29. VTR of Water in Vapor Transfer Studies for Blend Membranes

## Water Effective Permeability ( $P_{eff}$ )

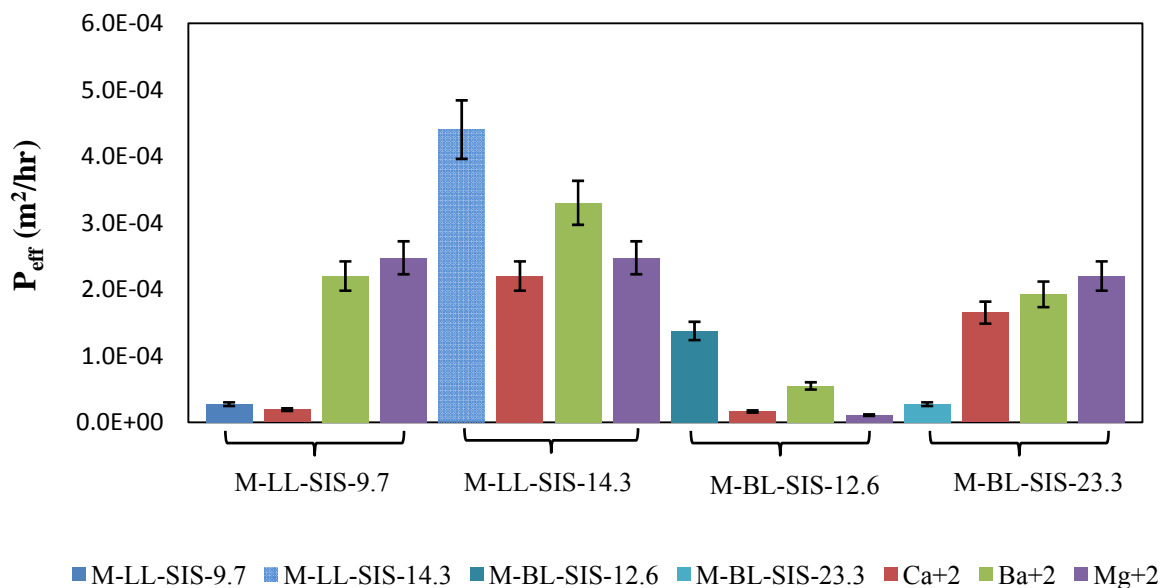
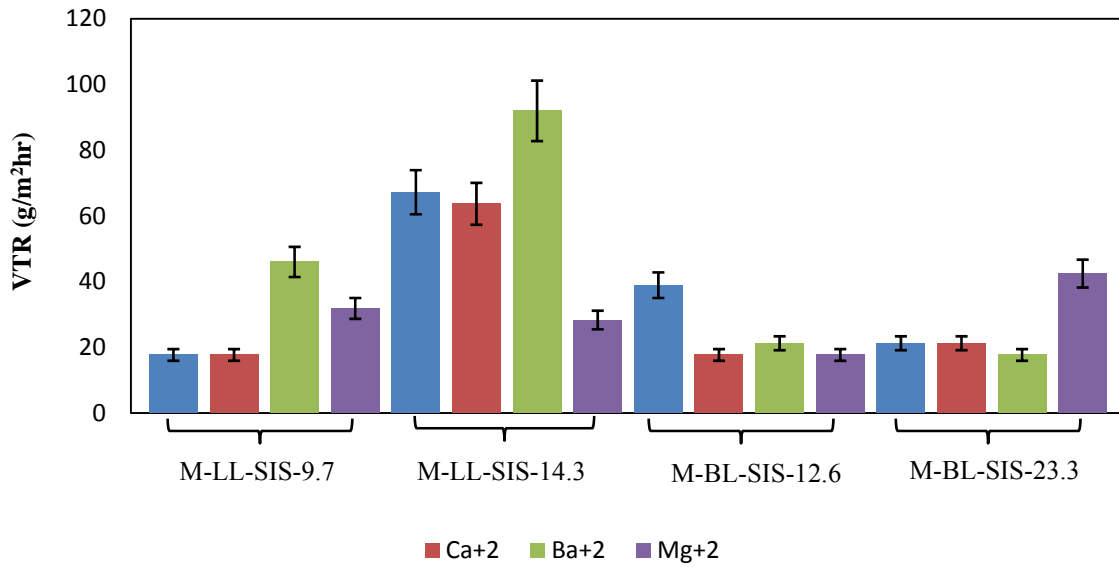


Figure 30.  $P_{eff}$  of Water in Vapor Transfer Studies for Blend membranes

## DMMP Vapor Transfer Rate (VTR)



**Figure 31. VTR of DMMP in Vapor Transfer Studies for Blend Membranes**

## DMMP Effective Permeability ( $P_{eff}$ )

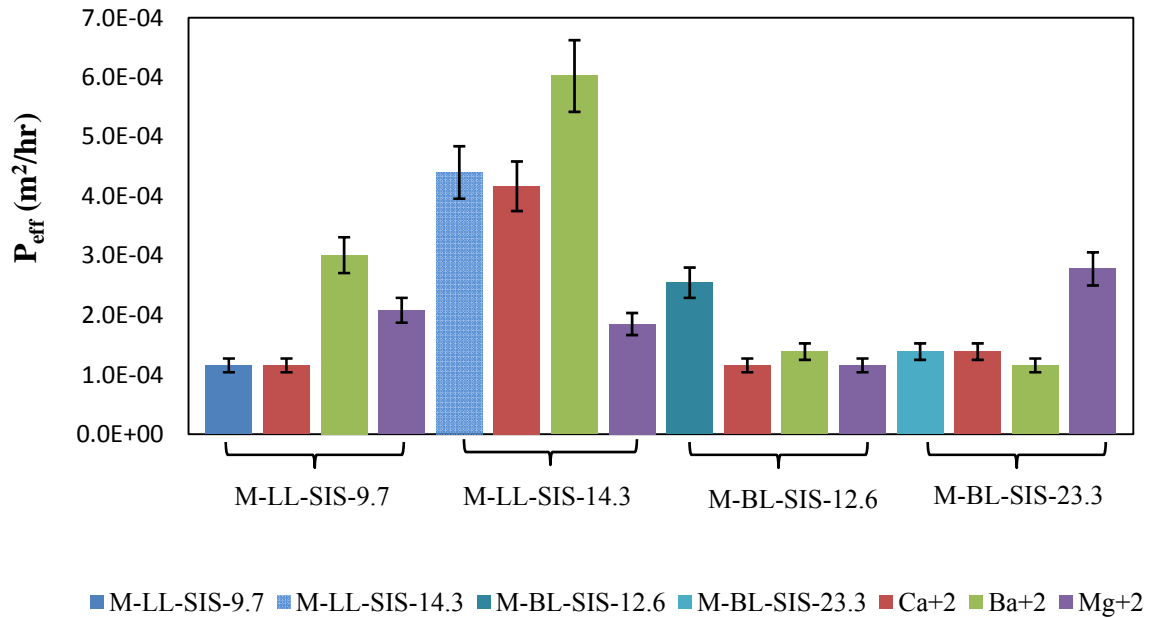


**Figure 32.  $P_{eff}$  of DMMP in Vapor Transfer Studies for Blend membranes**

### 5.4.2 Selectivity

A membrane with high water transport not necessarily shows the lowest DMMP transfer. For that reason, to get a more accurate selection, selectivity calculations were made using the following equation

$$\alpha = \frac{P_{eff (water)}}{P_{eff (DMMP)}}$$

Results in Figure 33 show a better performance for the cross-linked membranes obtaining selectivity values up to approximately 1.7, which is not bad considering the low sulfonation levels for these membranes. Selectivities of that magnitude can be used in other applications, like specialty separation processes, where efficiency can be increased using more membrane layers or multi-stage processes, but not specifically in the chemical and biological protective clothing application.

As discussed in Section 5.4.1, the best material is the one that blocks toxic agents and at the same time allows water to escape. Taking that into consideration, these low values of selectivities show the opposite. This means that the selectivity goes in the other direction.

## Selectivity

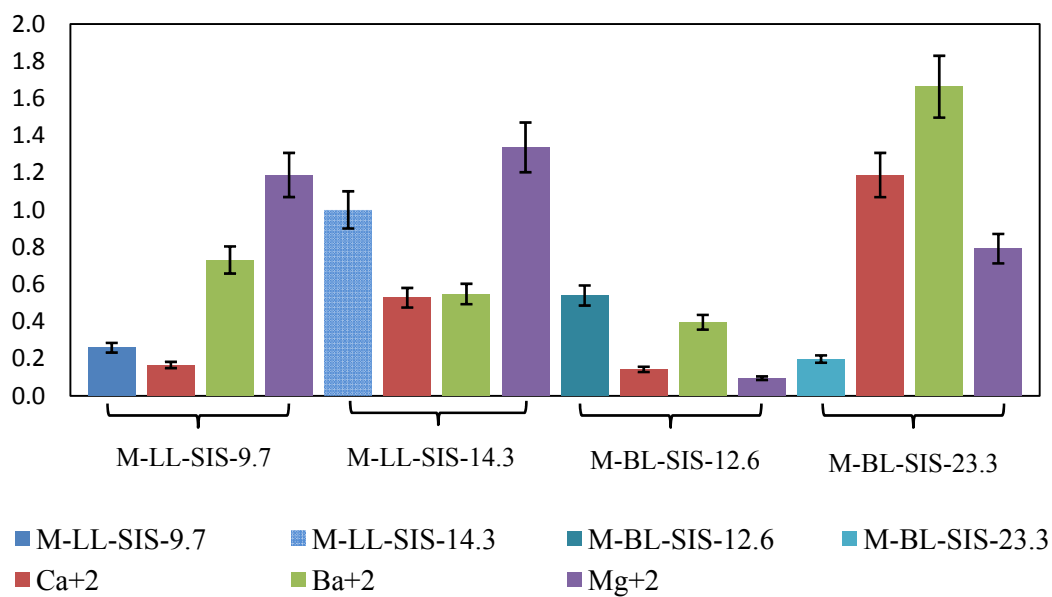


**Figure 33. Selectivity between Water and DMMP Vapor Transport Studies**

## 5.5 FT-IR Spectroscopy

Infrared spectroscopy detects sulfonic groups and the cation effects of the cross-linked membranes. Peak intensity can be an accurate measure of the amount of sulfonation. As shown in Figures 34 and 35, sulfonic groups appear in two different regions regardless of the difference between linear and branched morphologies. The first region, in the range of  $1430 - 1330 \text{ cm}^{-1}$ , is attributed to the asymmetric stretching vibration of the two S=O bonds in the sulfonate functional group. Sulfonate molecules contain one  $\text{SO}_2$  group (equivalent to two S=O bonds) and one S-O single bond. The second region, that appears from  $1340 - 1310 \text{ cm}^{-1}$ , is also due to the asymmetric  $\text{SO}_2$  stretch but this time of the sulfone functional group. Sulfone molecules contain C-S bonds and the  $\text{SO}_2$  group [41].

Cations interactions with the sulfonic groups are notable comparing the peak intensities in the M-LL-SIS-30-9.7 and M-BL-SIS-30-12.6 FT-IR spectrums (Figures 36 & 37). Reductions in peak intensities are attributed to the stabilization of the chemical charges between the cations and the oxygen molecules of the sulfonic groups.

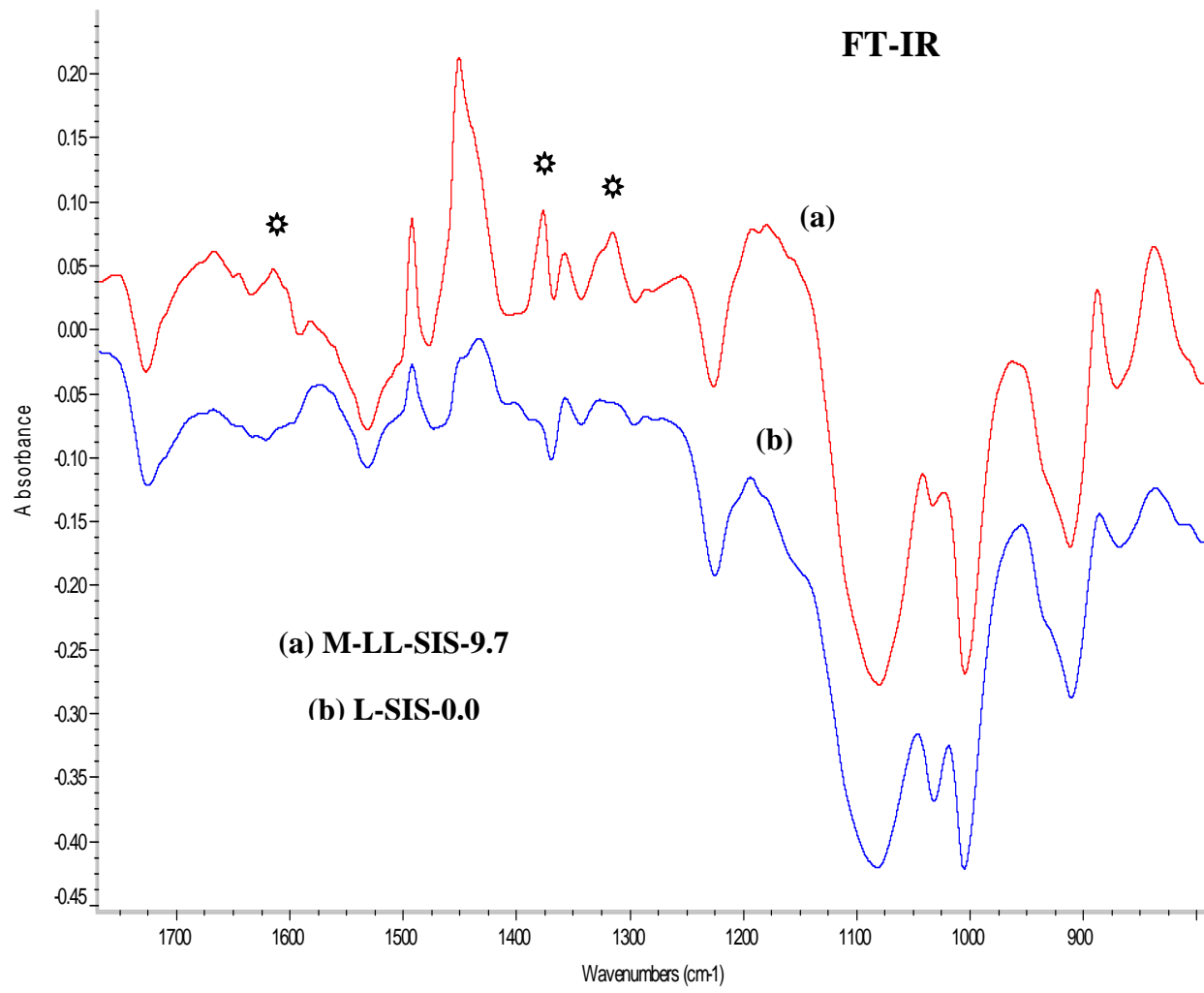


**Figure 34. FT-IR Spectrums for linear blend M-LL-SIS-9.7 and unsulfonated L-SIS-0.0**

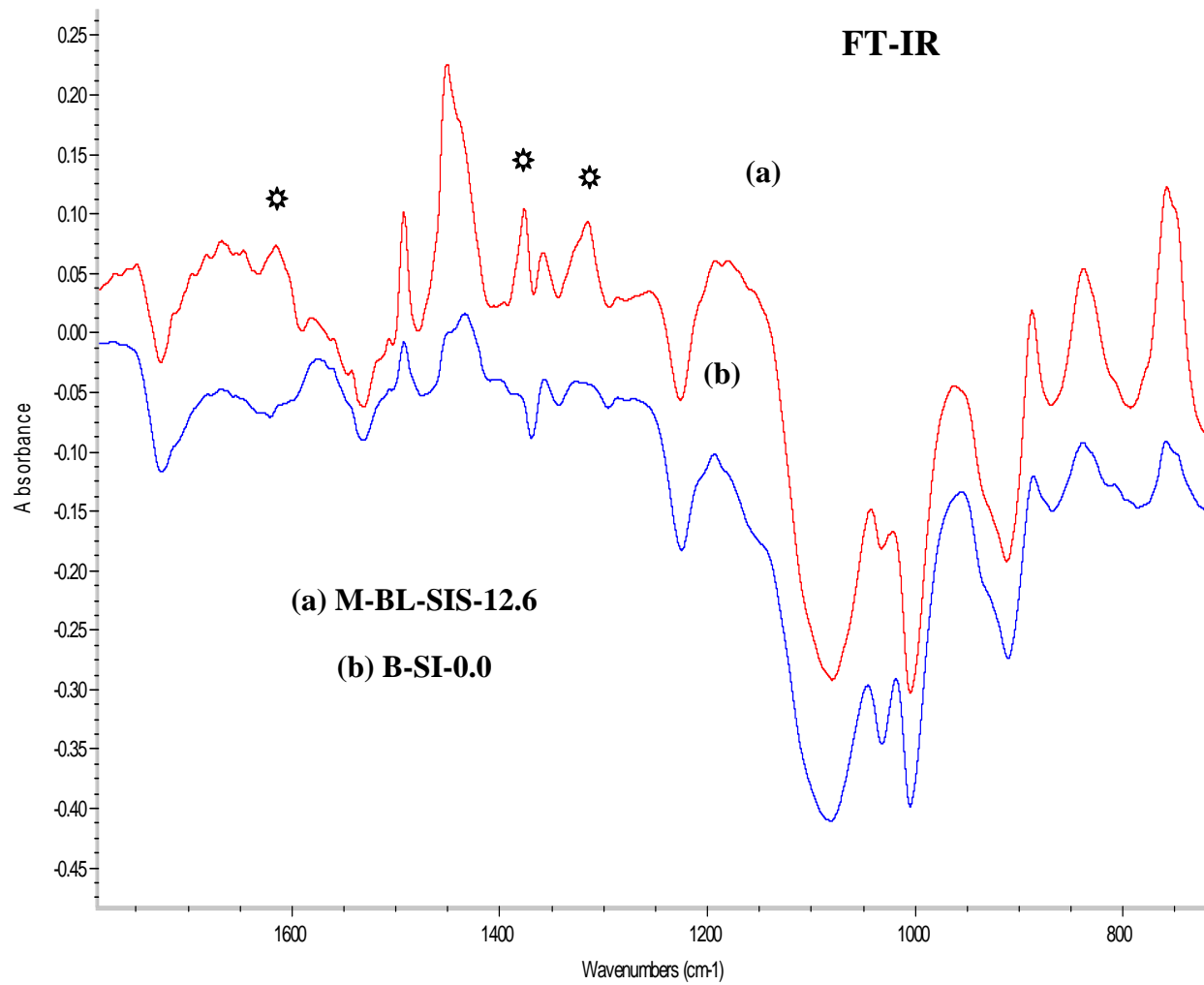


**Figure 35. FT-IR Spectrums for branched blend M-BL-SIS-12.6 and unsulfonated B-SI-0.0**

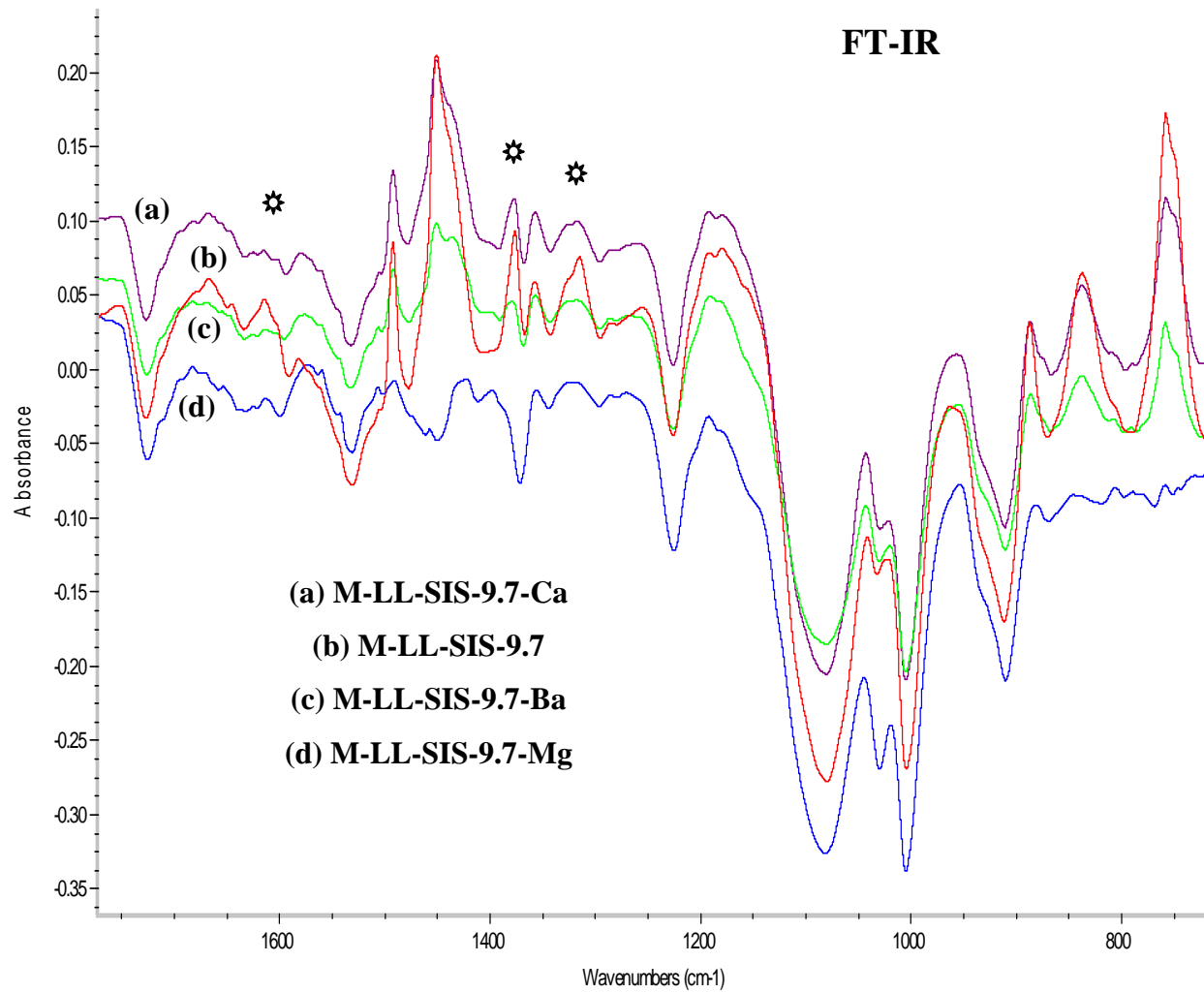


**Figure 36. FT-IR Spectrums for branched blend M-LL-SIS-9.7 and cross-linked with  $\text{Ca}^{+2}$ ,  $\text{Ba}^{+2}$ ,  $\text{Mg}^{+2}$**

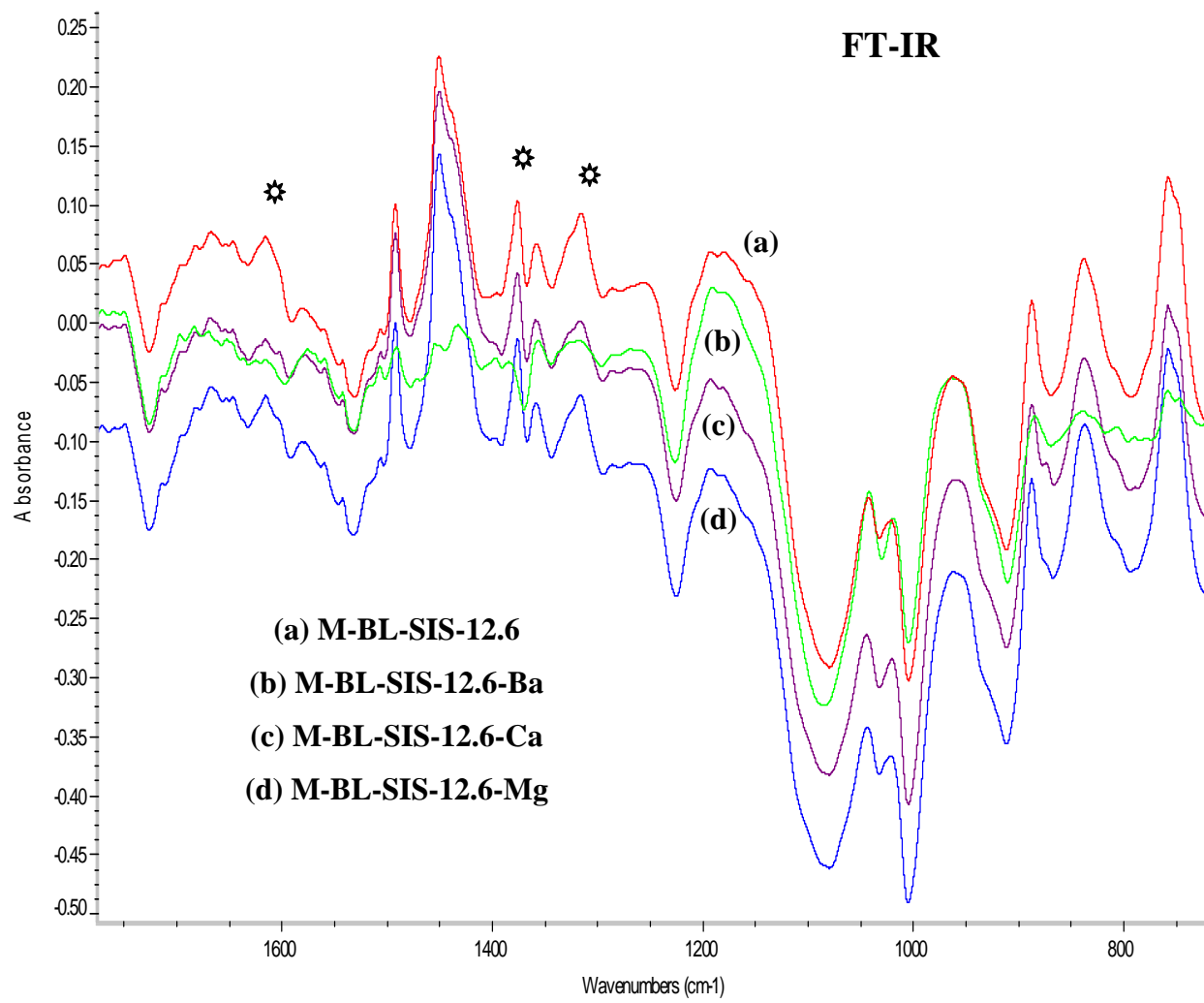


**Figure 37. FT-IR Spectrums for branched blend M-BL-SIS-12.6 and cross-linked with Ca<sup>+2</sup>, Ba<sup>+2</sup>, Mg<sup>+2</sup>**

## 5.6 Small Angle X-Ray Scattering (SAXS)

### 5.6.1 SAXS Form Factor

The scattering of one particle in a sample, which is made of many atoms, can be explained as the interference pattern produced by all the waves that are sent to the detector from every electron/atom inside the particle. Summing up all the wave amplitudes at the detector position, and making the square of this sum, results in a scattering or interference pattern. This pattern oscillates in a fashion that is characteristic for the shape or the form of the particle and therefore is called the form factor because it must be scaled with a constant in order to match the experimental intensity units.

### 5.6.2 SAXS Structure Factor

The interference pattern also considers distance contributions from neighboring particles of large molecules. This additional interference pattern will be multiply with the form factor of the single particles to obtain the structure or lattice factor. In SAXS curves, concentration effects become visible at small angles by the formation of a descent in intensity and a small overshoot at the edge. This overshoot can develop into a pronounced peak when the particles or atoms align themselves into a highly ordered and periodic arrangement. That concept is called Bragg peak and is represented with a maximum ( $q_{Bragg}$ ) in the SAXS curves that indicated the distance ( $d_{Bragg}$ ) between the aligned particles.  $d_{Bragg}$  was calculated with the Bragg's law using the following equation

$$d_{Bragg} = \frac{2\pi}{q_{Bragg}}.$$

Investigating the power law of the form factor at small angles helps to classify different shapes (globular, cylindrical and lamellar) as shown in Figure 38. In a double logarithmic plot and initial slope of 0, -1 or -2 indicates globular, cylindrical or lamellar shape, respectively. If the slope is steeper than that then the particles are too big to be resolved [44].

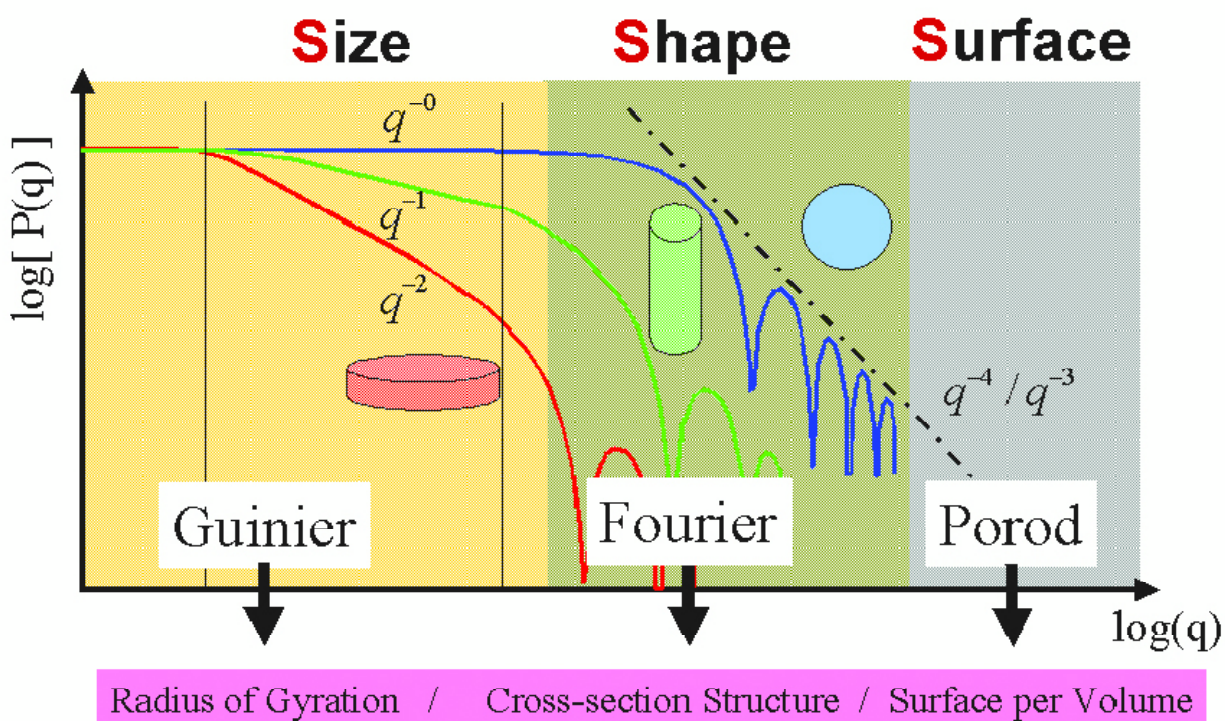


**Figure 38. Domains of a particle form factor**

Figures 39 & 40 of sulfonated branched and linear polymers, respectively, present different types of domains and arrangements with increasing the sulfonation level. At low sulfonation levels the slope of the logarithmic SAXS plot is much steeper than the slope at higher sulfonation levels.

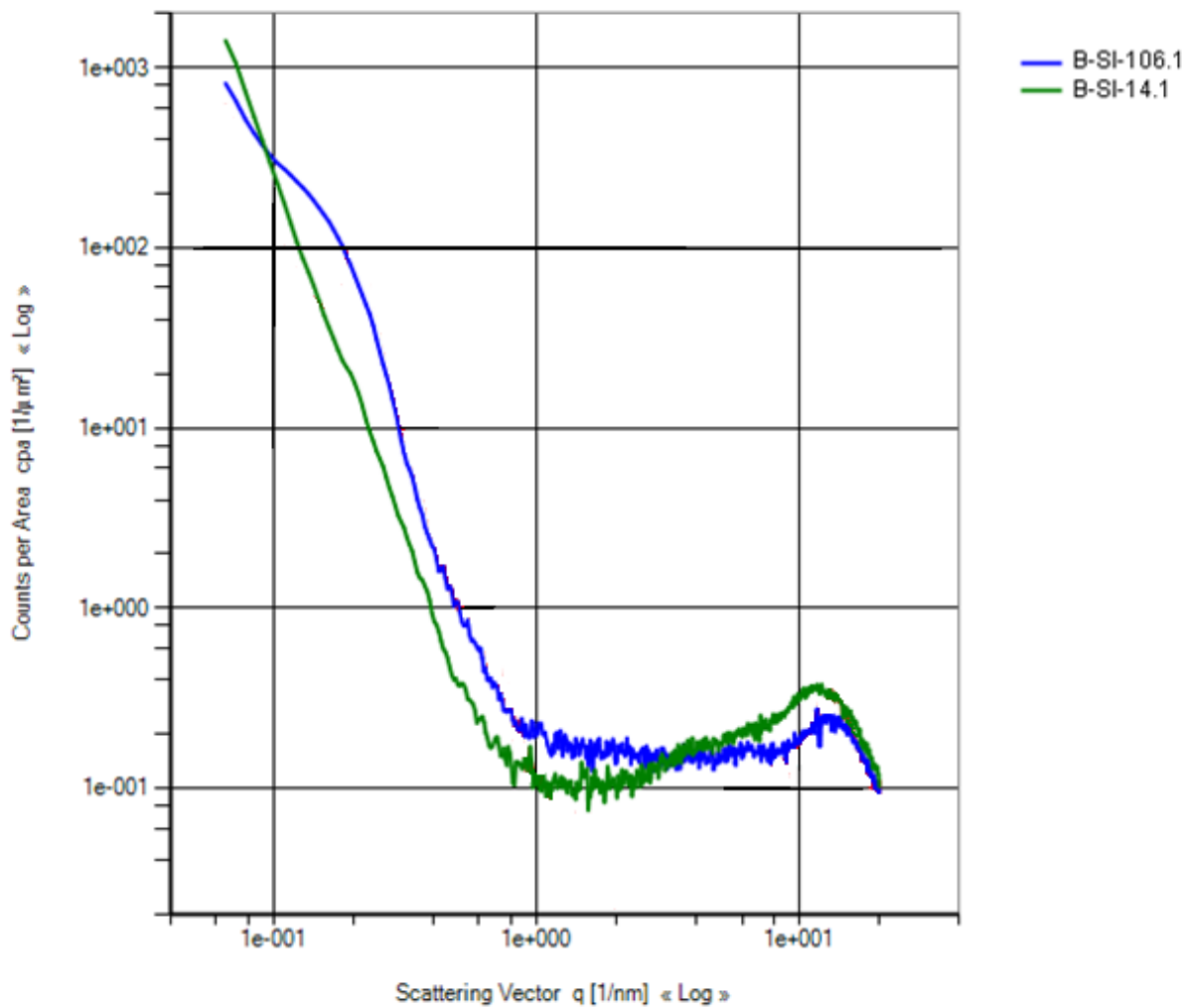


**Figure 39. Logarithmic SAXS Profile for B-SI-106.1 and B-SI-14.1**

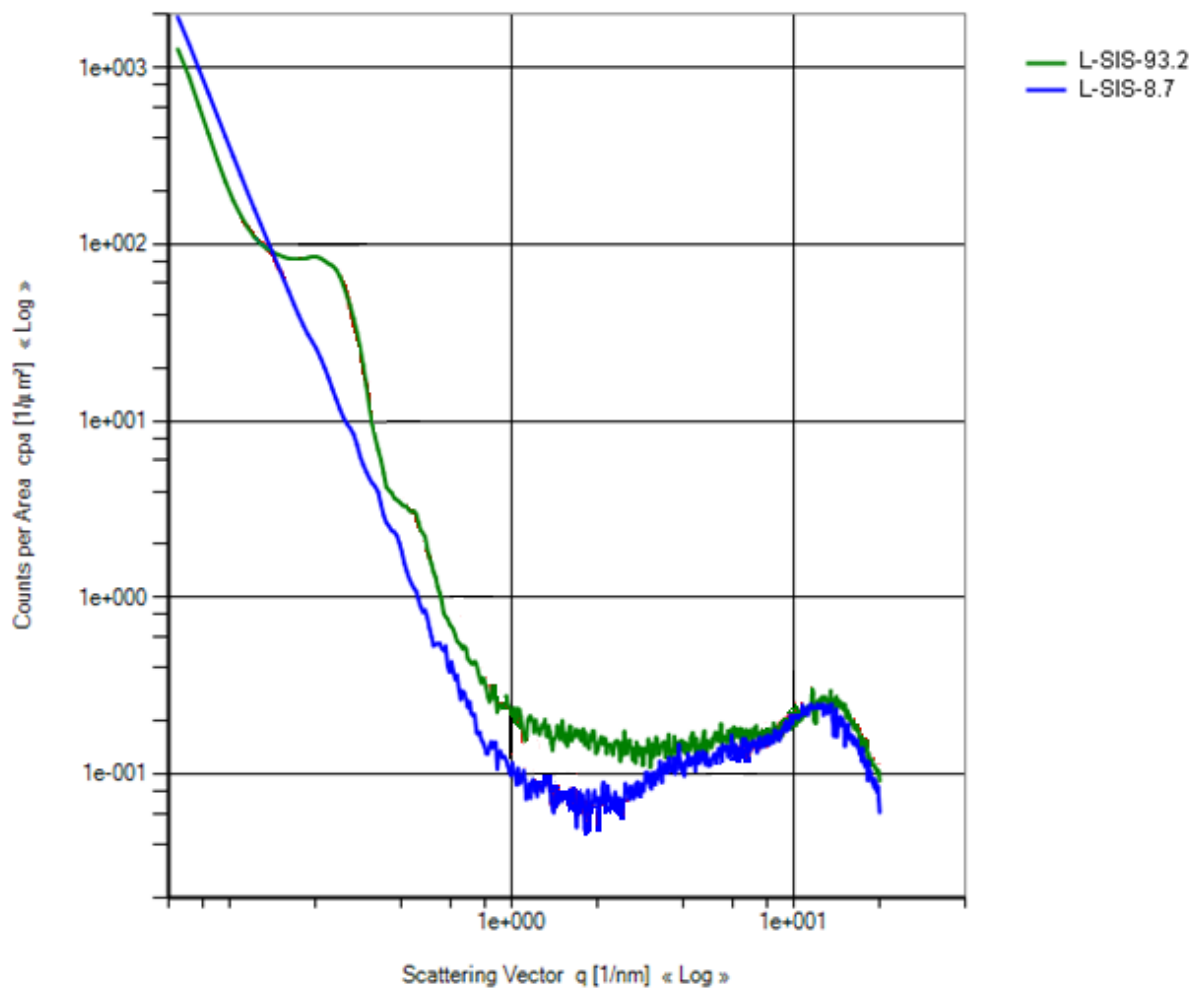


**Figure 40. Logarithmic SAXS Profile for L-SIS-93.2 and LB-SIS-9.7**

Blends SAXS curves were presented in Figures 41-44. The distance between align particles were obtained for each sulfonated and cross-linked blend and presented in Table 6.

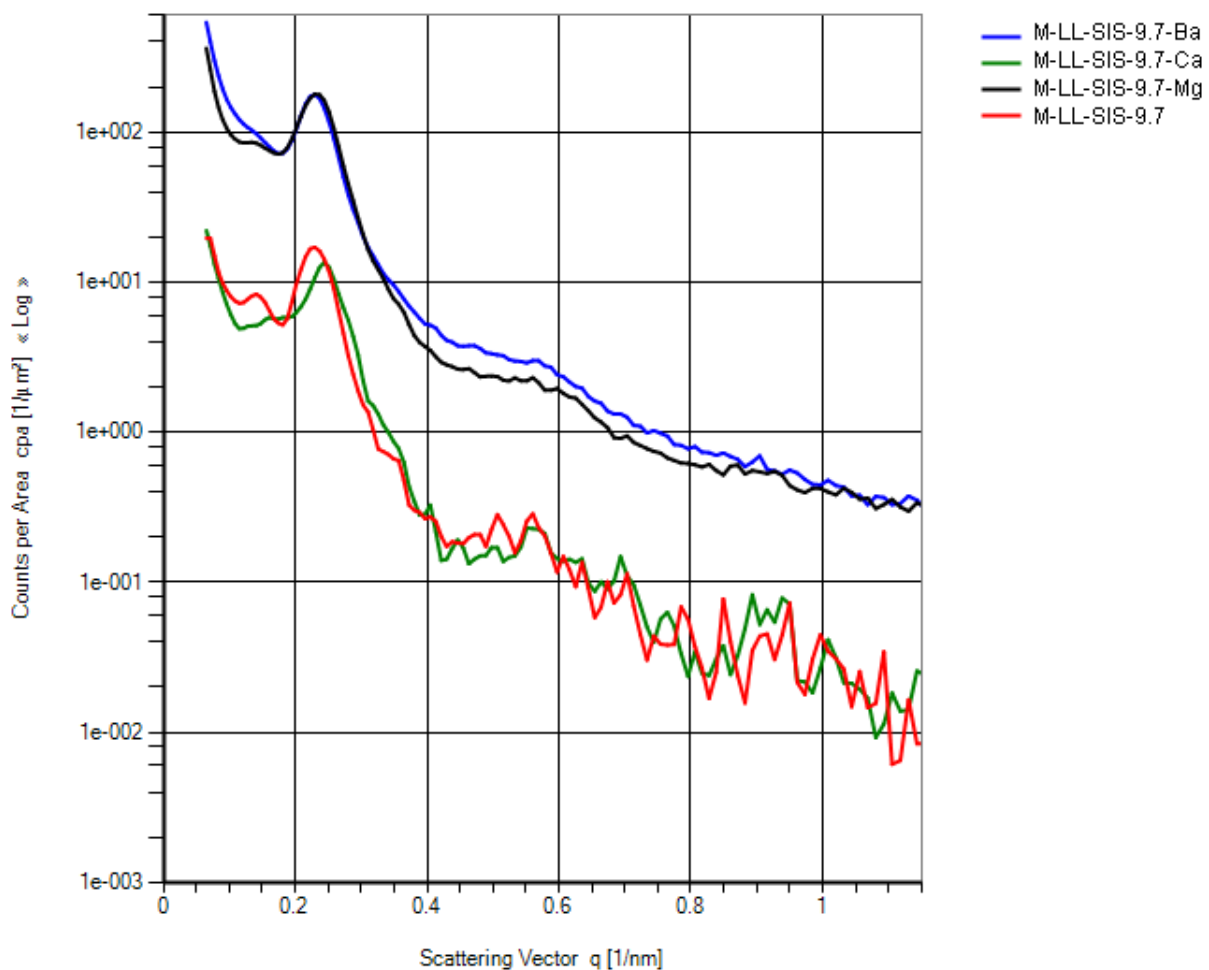


**Figure 41. SAXS Profile for blends M-LL-SIS-9.7, M-LL-SIS-9.7-Ba, M-LL-SIS-9.7-Ca and M-LL-SIS-9.7-Mg**

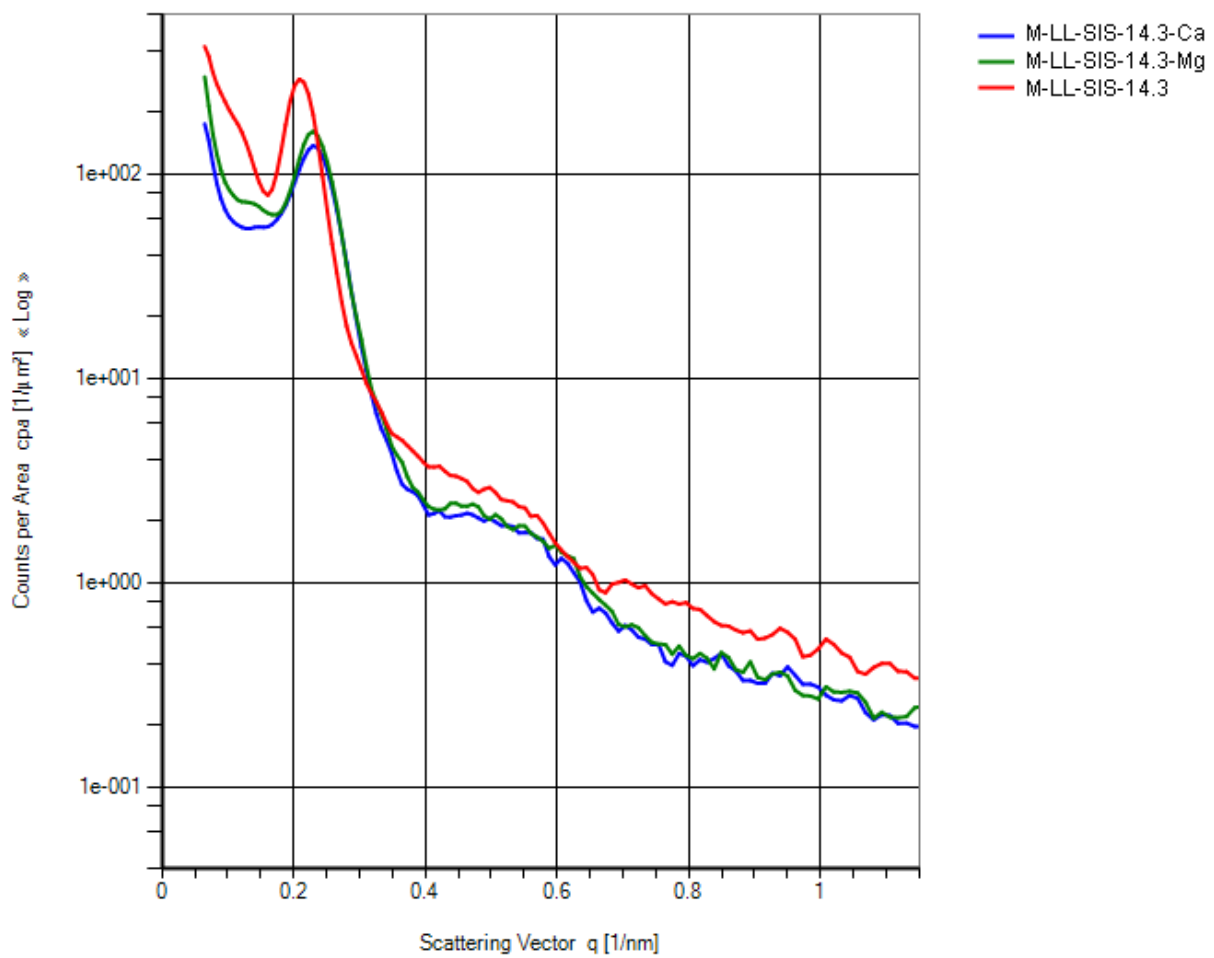


**Figure 42. SAXS Profile for blends M-LL-SIS-14.3, M-LL-SIS-14.3-Ba, M-LL-SIS-14.3-Ca and M-LL-SIS-14.3-Mg**

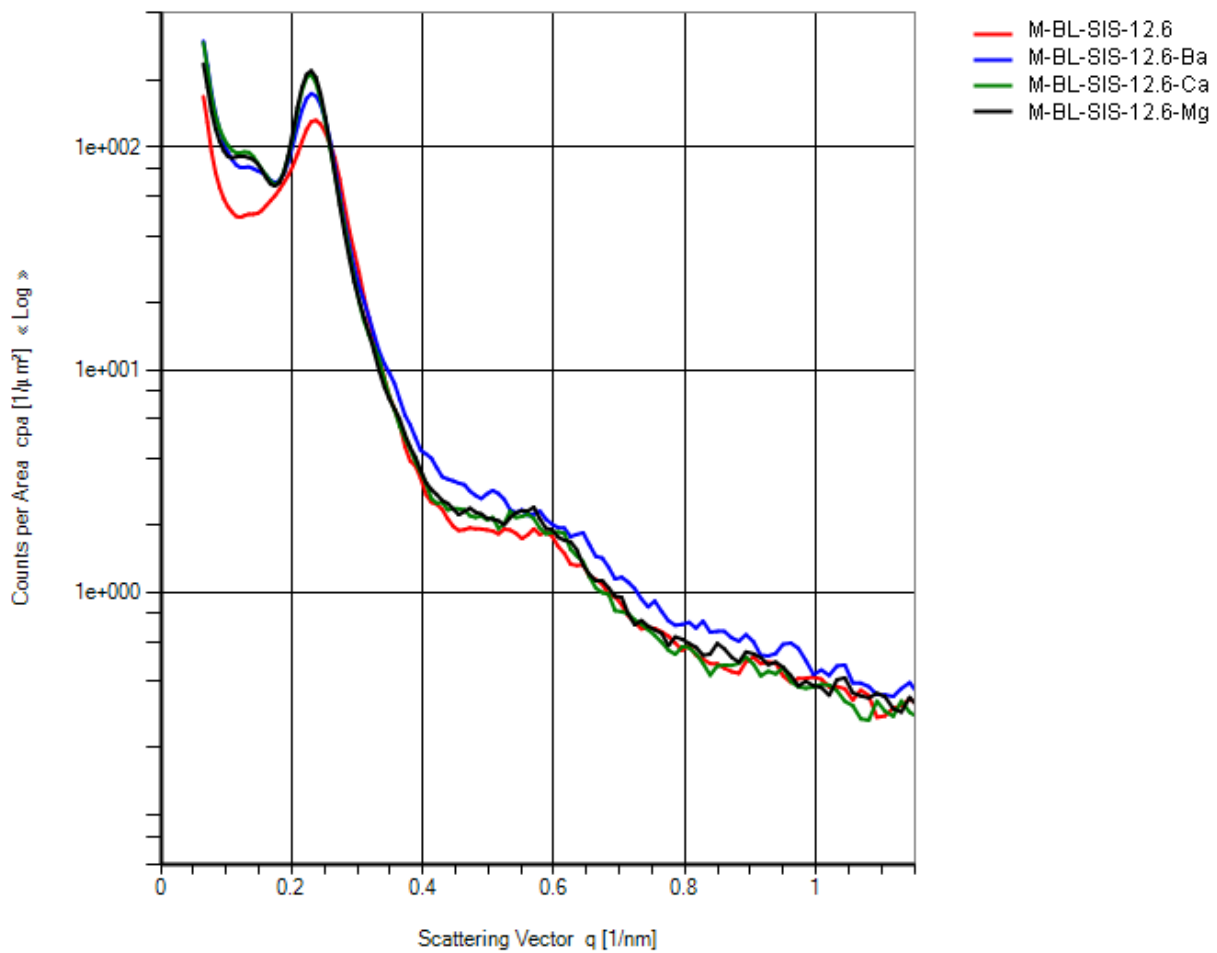


**Figure 43. SAXS Profile for blends M-BL-SIS-12.6, M-BL-SIS-12.6-Ba, M-BL-SIS-12.6-Ca and M-BL-SIS-12.6-Mg**

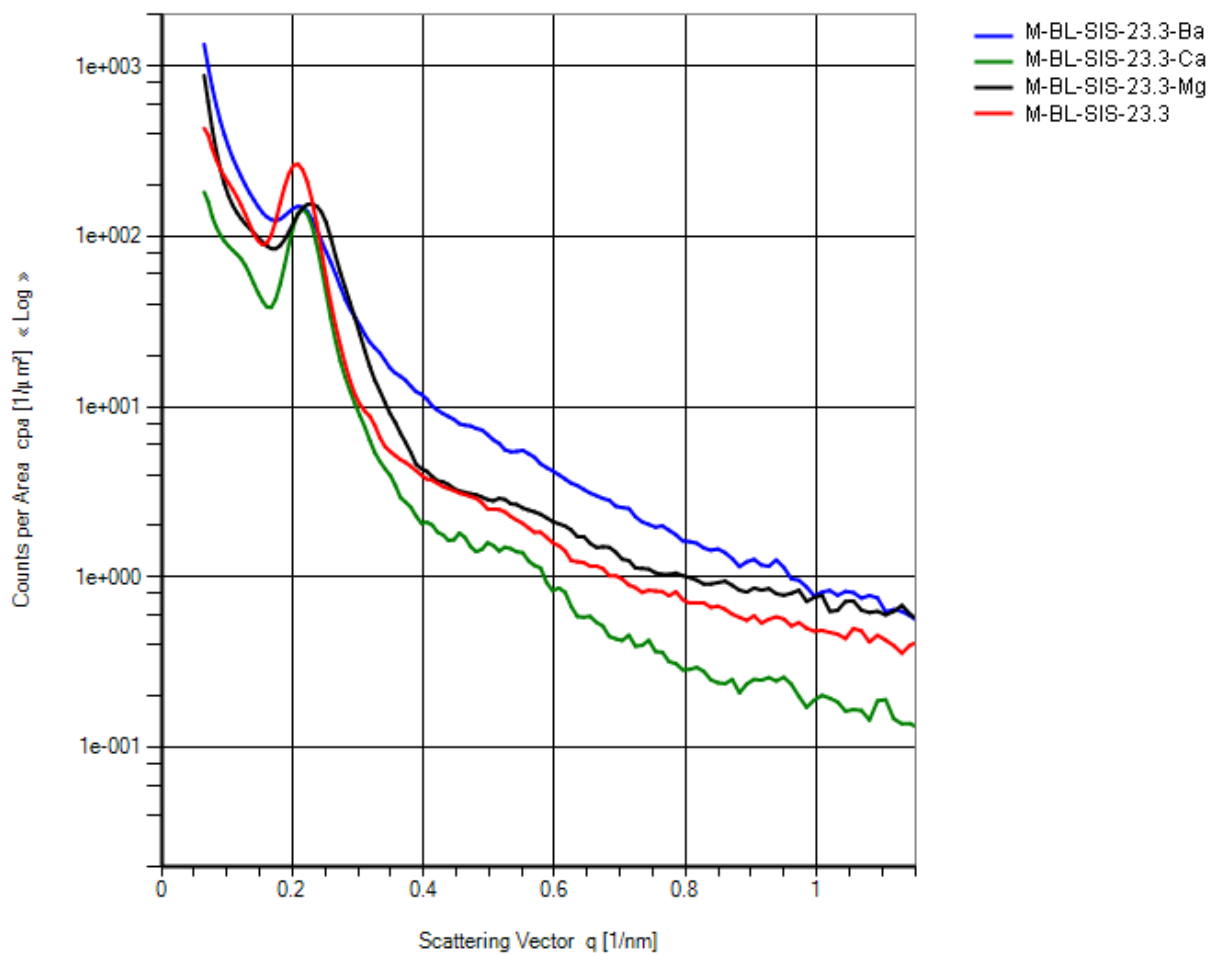


**Figure 44. SAXS Profile for blends M-BL-SIS-23.3, M-BL-SIS-23.3-Ba, M-BL-SIS-23.3-Ca and M-BL-SIS-23.3-Mg**

Blend	$d_{Bragg}$ (nm)
M-LL-SIS-9.7	27.9
M-LL-SIS-9.7-Ba	27.9
M-LL-SIS-9.7-Ca	25.1
M-LL-SIS-9.7-Mg	27.3
M-LL-SIS-14.3	29.9
M-LL-SIS-14.3-Ba	-
M-LL-SIS-14.3-Ca	27.3
M-LL-SIS-14.3-Mg	27.3

Blend	$d_{Bragg}$ (nm)
M-BL-SIS-12.6	26.7
M-BL-SIS-12.6-Ba	27.3
M-BL-SIS-12.6-Ca	27.6
M-BL-SIS-12.6-Mg	27.6
M-BL-SIS-23.3	30.6
M-BL-SIS-23.3-Ba	29.9
M-BL-SIS-23.3-Ca	29.2
M-BL-SIS-23.3-Mg	27.3

**Table 6. Bragg distance for linear and branched blends**

## 5.7 Scanning Electron Microscope (SEM)

The SEM was used to view and analyze the solid surface of the nanostructured membranes. Figure 45 shows the range of applicability of different characterization techniques including the SEM and SAXS. SEM is in the range of approximately 50 nm to 1 mm. In spite of that, samples were analyzed to see, if possible, the morphological changes and the nanochannels created after sulfonation. Images were obtained until 10  $\mu\text{m}$  of magnification and that is not enough to view the nanochannels of the sulfonated membranes. SEM images were presented in Figure 46. At 200  $\mu\text{m}$  of magnification can be seen some type of arrangement due to the phase segregation of the PS and PI blocks.

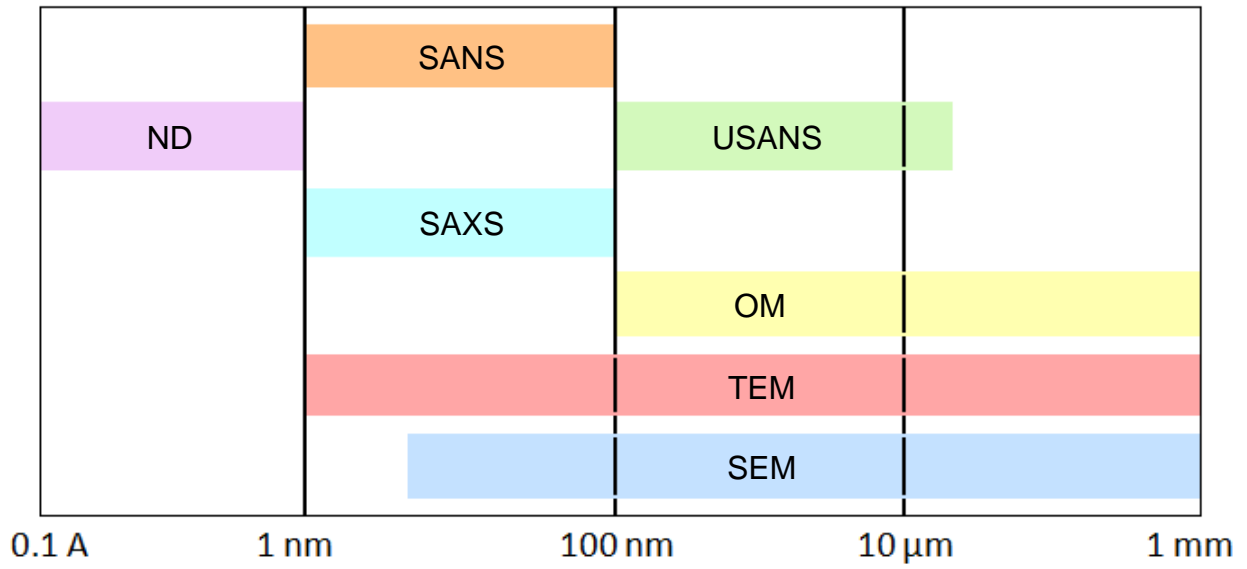


**Figure 45. Range of Applicability of different Characterization Techniques**

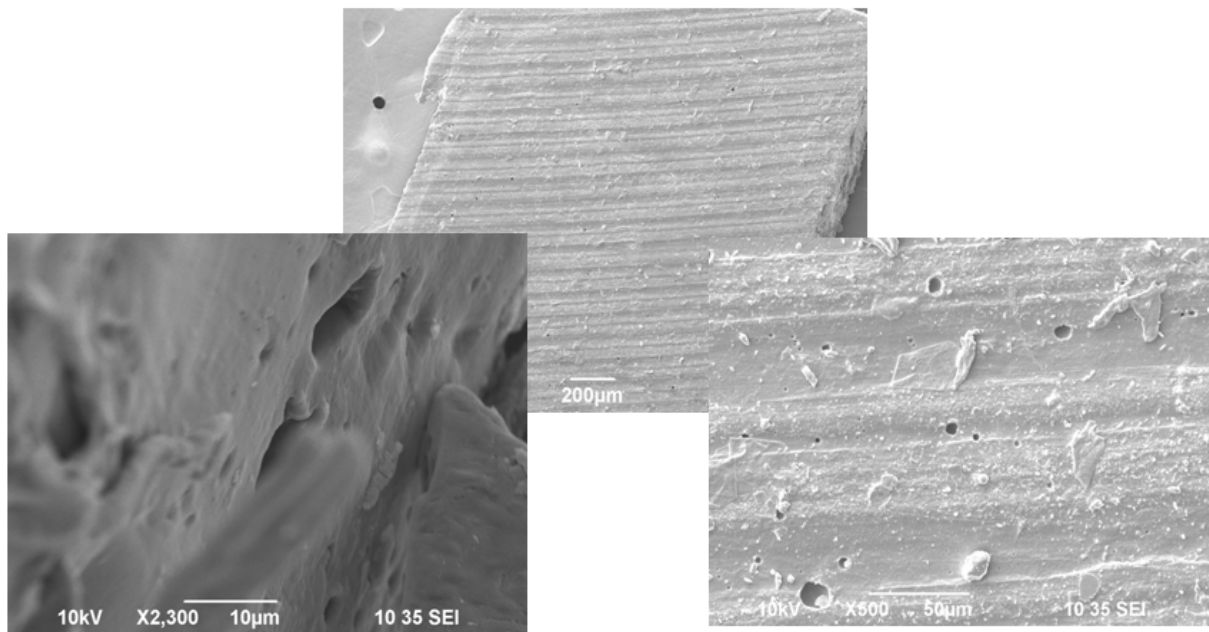


**Figure 46. SEM images of the nanostructured membranes**

## 6 Conclusions and Recommendations

In this study, poly(styrene-isoprene-styrene) was sulfonated at different sulfonation levels and blends were prepared to recover the elastomeric properties of the sulfonated linear SIS and branched SI polymers. Synthesis of poly(styrene-isoprene-styrene) (SIS) is significantly different from poly(styrene-isobutylene-styrene) (SIBS) primarily for the unsaturated bonds in isoprene block. Unsulfonated L-SIS and B-SI behave very similar; however, sulfonated L-SIS and B-SI show tremendous potential as proton exchange membranes or selective permeable membranes for different separations processes. Different sulfonation levels and blends of sulfonated and unsulfonated linear/branched polymers resulted in unique morphologies capable of selective separations.

TGA results of the membranes show thermal stability up to 440°C and confirm sulfonation obtained from elemental analysis. Sulfonation reaction increased transport properties and the polymer thermal stability. Also, sulfonic groups were confirmed with the water swelling experiments and the infrared spectroscopy analysis.

A further analysis of the cation interactions will be necessarily for a better understanding of the membranes behaviors. Study the size, charge and energetic environment of each cation with the sulfonic groups and analyze the molecular interaction with the sulfonated membranes are also very important things. A powerful technique with a higher resolution will be needed to view the nanostructures and morphologies of the sulfonated membranes.

## 7 References

- [1] N. Carretta, V. Tricoli, F. Picchioni, Ionomeric membranes based on partially sulfonated poly(styrene): synthesis, proton conduction and methanol permeation, *J. Membrane Sci.* 166 (2000) 189-197.
- [2] P. Raghu, C. K. Nere, R. N. Jagtap, Effect of Styrene-Isoprene-Styrene, Styrene-Butadiene-Styrene, and Styrene-Butadiene Rubber on the Mechanical, Thermal, Rheological, and Morphological Properties of Polypropylene/Polystyrene Blends, *J. Appl. Polym. Sci.* 88 (2003) 266–277.
- [3] Y. A. Elabd, E. Napadensky, Sulfonation and characterization of poly(styrene-isobutylene-styrene) triblock copolymers at high ion-exchange capacities, *Polym.* 45 (2004) 3037–3043.
- [4] K. A. Kreuer, On the development of proton conducting polymer membranes for hydrogen and methanol fuel cells, *J. Membr. Sci.* 185 (2001) 3.
- [5] K. A. Kreuer, On the development of proton conducting materials for technological applications, *Solid State Ionics* 97 (1997) 1.
- [6] X. Jin, M. T. Bishop, T. S. Ellis, F. Karasz, A sulphonated poly(aryl ether ketone), *Br. Polym. J.* 17 (1985) 4.
- [7] T. Kobayashi, M. Rikukawa, K. Sanui, N. Ogata, Proton-conducting polymers derived from poly(ether-etherketone) and poly(4-phenoxybenzoyl-1,4-phenylene), *Solid State Ionics* 106 (1998) 219.
- [8] S. M. J. Zaidi, S. D. Mikailenko, G. P. Robertson, M. D. Guiver, S. Kaliaguine, Proton conducting composite membranes for polyether ether ketone and heteropolyacids for fuel cell applications, *J. Membr. Sci.* 173 (2000) 17.
- [9] S. D. Mikhailenko, S. M. J. Zaidi, S. Kaliaguine, Sulfonated polyether ether ketone composite polymer electrolyte membranes, *Catal. Today* 67 (2001) 225.
- [10] V. Silva, B. Ruffmann, H. Silva, A. Mendes, M. Madeira, S. Nunes, Zirconium oxide modified sulfonated poly(ether ether ketone) membranes for direct methanol fuel cell applications, *Mater. Sci. Forum* 455–456 (2004) 587.
- [11] J. Kerres, W. Zhang, L. Jorissen, V. Gogel, Application of different types of polyarylblend-membranes in DMFC, *J. New Mater. Electrochem. Syst.* 5 (2002) 97.
- [12] G. Alberti, M. Casciola, L. Massinelli, B. Bauer, Polymeric proton conducting membranes for medium temperature fuel cells (110–160 °C), *J. Membr. Sci.* 185 (2001) 73.

- [13] V. S. Silva, B. Ruffmann, S. Vetter, A. Mendes, L. M. Madeira, S. P. Nunes, Characterization and application of composite membranes in DMFC, *Catal. Today* 104 (2005) 205–212.
- [14] M. L. Ponce, L. Prado, B. Ruffmann, K. Richau, R. Mohr, S. P. Nunes, Reduction of methanol permeability in polyetherketone–heteropolyacid membranes, *J. Membr. Sci.* 217 (2003) 5.
- [15] S. P. Nunes, B. Ruffmann, E. Rikowsky, S. Vetter, K. Richau, Inorganic modification of proton conductive polymer membranes for direct methanol fuel cells, *J. Membr. Sci.* 203 (2002) 215.
- [16] C. Manea, M. Mulder, Characterization of polymer blends of polyethersulfone/sulfonated polysulfone and polyethersulfone/sulfonated polyetheretherketone for direct methanol fuel cell applications, *J. Membr. Sci.* 206 (2002) 443.
- [17] V. S. Silva, A. Mendesa, L. M. Madeira, S. P. Nunes, Proton exchange membranes for direct methanol fuel cells: Properties critical study concerning methanol crossover and proton conductivity, *J. of Membr. Sci.* 276 (2006) 126–134.
- [18] M. H. Yildirim, D. Stamatialis, M. Wessling, Dimensionally stable Nafion–polyethylene composite membranes for direct methanol fuel cell applications, *J. of Membr. Sci.* 321 (2008) 364–372.
- [19] B. Jung, B. Kim, J. M. Yang, Transport of methanol and protons through partially sulfonated polymer blend membranes for direct methanol fuel cell, *J. of Membr. Sci.* 245 (2004) 61–69.
- [20] D. M. Crawford, E. Napadensky, N. C. B. Tana, D. A. Reuschleb, D. A. Mountzb, K. A. Mauritzb, K. S. Laverdurec, S. P. Gidoc, W. Liud, B. Hsiaod, Structure/property relationships in polystyrene-polyisobutylene-polystyrene block copolymers, *Thermochim. Acta.* 367-368 (2001) 125-134.
- [21] D. Suleiman, Y. A. Elabd, E. Napadensky, J. M. Sloan, D. M. Crawford, Thermogravimetric characterization of sulfonated poly(styrene-isobutylene-styrene) block copolymers: effects of processing conditions, *Thermochim. Acta.* 430 (2005) 149–154.
- [22] E. Napadensky, D. Crawford, J. Sloan, N. B. Tan, Viscoelastic and Transport Properties of Sulfonated PS-PIB-PS Block Copolymers, *ARL-TR-2482*, US Army Research Laboratory, Aberdeen Proving Ground, MD, May 2001.
- [23] E. Napadensky, Y. A. Elabd, Breathability and Selectivity of Selected Materials for Protective Clothing, *ARL-TR-3235*, US Army Research Laboratory, Aberdeen Proving Ground, MD, July 2004.

- [24] A. Jonquieres, R. Clement, P. Lochon, Permeability of block copolymers to vapors and liquids, *Prog. Polym. Sci.* 27 (2002) 1803–1877.
- [25] N. Hadjichristidis, S. Pispas, G. Floudas, *Block Copolymers*, John Wiley & Sons, Inc., 2003.
- [26] S. Swier, V. Ramanib, J. M. Fenton, H. R. Kunz, M. T. Shaw, R. A. Weiss, Polymer blends based on sulfonated poly(ether ketone ketone) and poly(ether sulfone) as proton exchange membranes for fuel cells, *J. of Membr. Sci.*, 256 (2005) 122–133.
- [27] T. A. Zawodzinski, M. Neeman, L. O. Sillerud, S. Gottesfeld, Determination of water diffusion coefficients in perfluorosulfonate ionomeric membranes, *J. Phys. Chem.* 95 (1991) 6040.
- [28] M. Eikerling, A. A. Kornyshev, A. M. Kuznetsov, J. Ulstrup, S. Walbran, Mechanisms of proton conductance in polymer electrolyte membranes, *J. Phys. Chem.* 105 (2001) 3646.
- [29] L. Carrette, K. A. Friedrich, U. Stimming, Fuel cells – fundamentals and applications, *Fuel Cells* 1 (2001) 5–39.
- [30] P. Costamagna, S. Srinivasan, Quantum jumps in the PEMFC science and technology from the 1960s to the year 2000. Part II. Engineering, technology development and application aspects, *J. Power Sources* 102 (2001) 253–269.
- [31] K. Rikukawa, K. Sanui, Proton-conducting polymer electrolyte membranes based on hydrocarbon polymers, *Prog. Polym. Sci.* 25 (2000) 1463–1502.
- [32] D. J. Jones, J. Roziere, Recent advances in the functionalisation of polybenzimidazole and polyetherketone for fuel cell applications, *J. Membr. Sci.* 185 (2001) 41–58.
- [33] M. Montoya, J. P. Tomba, J. M. Carella, M. I. Gobernado-Mitre, Physical characterization of commercial polyolefinic thermoplastic elastomers, *European Polymer Journal* 40 (2004) 2757–2766.
- [34] C. Heitner-Wirguin, Recent advances in perfluorinated ionomer membranes: structure, properties and applications, *J. of Membr. Sci.* 120 (1996) 1–33.
- [35] B. L. Lee, T. W. Yang, E. Wilusz, Moisture Effects on Isobutylene-Isoprene Copolymer-Based Composite Barrier. I: Moisture Diffusion and Detection, *Polym. Eng. Sci.* 36 (1996) 1217-1231.
- [36] H. Bruschke, Industrial application of membrane separation processes, *Pure & App. Chem.*, 67, 6, (1995) 993-1002.

- [37] S. J. Taylor, R. F. Storey, J. G. Kopchick, K. A. Mauritz, Poly[(styrene-co-p-methylstyrene)-b-isobutylene-b-(styrene-co-pmethylstyrene)] triblock copolymers. 1. Synthesis and characterization, *Polymer* 45 (2004) 4719–4730.
- [38] L. Shao, T. S. Chung, G. Wensleyd, S. H. Gohb, K. P. Pramoda, Casting solvent effects on morphologies, gas transport properties of a novel 6FDA/PMDA–TMMDA copolyimide membrane and its derived carbon membranes, *J. of Membr. Sci.* 244 (2004) 77–87.
- [39] D. Suleiman, E. Napadensky, J.M. Sloan, D.M. Crawford, Thermogravimetric characterization of highly sulfonated poly(styrene-isobutylene-styrene) block copolymers: Effects of sulfonation and counter-ion substitution, *Thermochim. Acta.* 460 (2007) 35-40.
- [40] L. Szinicz, History of chemical and biological warfare agents, *Toxicology* 214 (2005) 167–181.
- [41] B. Smith, *INFRARED SPECTRAL INTERPRETATION: A Systematic Approach*, CRC Press, Boca Raton, Florida, 1999.
- [42] R. A. Nyquist, *INTERPRETING INFRARED, RAMAN, AND NUCLEAR MAGNETIC RESONANCE SPECTRA*, Volume 2, Academic Press, San Diego, CA, 2001.
- [43] G. Herzberg, *Infrared and Raman Spectra of Polyatomic Molecules*, Van Nostrand Reinhold: New York, 1945.
- [44] H. Schnablegger, Y. Singh, *A Practical Guide to SAXS Getting acquainted with the principles*, Anton Paar GmbH, Austria (2006).

# Appendices

## Appendix A

### A.1 Sulfonation Reaction Stoichiometric Calculations

SIS/SI

PS = 30%

$$\text{Moles PS} = gSIS \left( \frac{\frac{\%PS}{100}}{MW_{PS}} \right)$$

$$5gSIS \left( \frac{0.30gPS}{1gSIS} \right) \left( \frac{1molPS}{104.15gPS} \right) = 0.0144 \text{ moles PS}$$

**Acetyl Sulfate/Polymer Relation (2/1)**

$$2 * \text{Moles PS} = (2)(0.0144 \text{ moles PS}) = 0.1152 \text{ moles Acetyl Sulfate}$$

**Acetic Anhydride/Sulfuric Acid Relation (1:1)**

0.1152 moles Acetic Anhydride  $(CH_3CO)_2O$

0.1152 moles Sulfuric Acid  $(H_2SO_4)$

**Acetic Anhydride:**

$$V = \text{moles } (CH_3CO)_2O * \left( \frac{MW_{(CH_3CO)_2O}}{\rho_{(CH_3CO)_2O}} \right)$$

$$0.1152 \text{ moles } (CH_3CO)_2O \left( \frac{102.06g}{1mol(CH_3CO)_2O} \right) \left( \frac{mL}{1.08g} \right) = 10.89mL$$

**Sulfuric Acid:**

$$V = \text{moles } (H_2SO_4) * \left( \frac{MW_{(H_2SO_4)}}{\rho_{(H_2SO_4)}} \right)$$

$$0.1152 \text{ moles } (H_2SO_4) \left( \frac{98g}{1mol(H_2SO_4)} \right) \left( \frac{mL}{1.83g} \right) = 6.17mL$$

# Appendix B

## B.1 Elemental Analysis Results

**ATLANTIC MICROLAB, INC.**

Sample No. UPRM - 1 \* **SUBMITTER**

P.O. Box 2288  
Norcross, Georgia 30091  
(770) 242-0082  
**www.atlanticmicrolab.com**

PROFESSOR/SUPERVISOR: DAVID SULEIMAN NAME DAVID SULEIMAN DATE 04/21/2009  
P.O. #: \_\_\_\_\_

Company / School UNIVERSITY OF PUERTO RICO  
Address CHEMICAL ENGINEERING DEPARTMENT  
UNIVERSITY OF PUERTO RICO  
MAYAGUEZ, PUERTO RICO 00681-9046

Element	Theory	Found		Single <input checked="" type="checkbox"/> Duplicate <input type="checkbox"/>	
				Elements Present:	C S H O
C		85.93		Analyze for: C S H	
S		0.73		Hygroscopic <input checked="" type="checkbox"/> Explosive <input type="checkbox"/> M.P. <u>120 C</u> B.P. _____	
H		10.14		To be dried: Yes <input checked="" type="checkbox"/> No <input type="checkbox"/> Temp. <u>50 C</u> Vac. <input checked="" type="checkbox"/> Time _____	
O		2.34		FAX Service <input type="checkbox"/> EMAIL Service <input checked="" type="checkbox"/> FAX # /EMAIL <u>dsuleiman@uprm.edu</u>	
				Rush Service <input type="checkbox"/> (SEE CURRENT Phone Service <input type="checkbox"/> PRICE LIST) Phone No. _____	

Date Received JUL 14 2008 Date Completed JUL 15 2008  
Remarks: \_\_\_\_\_

**Figure B.1. Elemental Analysis Results from Atlantic Microlab, Inc.**



## Appendix C

### C.1 Water Swelling Data for sulfonated and cross-linked Blend Membranes

M-LL-SIS-9.7

<b>W<sub>membrane after oven</sub> (g)</b>	<b>W<sub>wet membrane</sub> (g)</b>	<b>t (hr)</b>	<b>Water Swelling Ratio</b>	<b>%</b>
0.0331	0.0331	0	0.0000	0.00
	0.0358	72	0.0816	8.16
	0.0360	96	0.0876	8.76
	0.0363	120	0.0967	9.67
	0.0364	144	0.0997	9.97
	0.0364	168	0.0997	9.97

M-LL-SIS-9.7-Ca

<b>W<sub>membrane after oven</sub> (g)</b>	<b>W<sub>wet membrane</sub> (g)</b>	<b>t (hr)</b>	<b>Water Swelling Ratio</b>	<b>%</b>
0.0276	0.0276	0	0.0000	0.00
	0.0298	72	0.0797	7.97
	0.0302	96	0.0942	9.42
	0.0305	120	0.1051	10.51
	0.0307	144	0.1123	11.23
	0.0307	168	0.1123	11.23

M-LL-SIS-9.7-Ba

<b>W<sub>membrane after oven</sub> (g)</b>	<b>W<sub>wet membrane</sub> (g)</b>	<b>t (hr)</b>	<b>Water Swelling Ratio</b>	<b>%</b>
0.0356	0.0356	0	0.0000	0.00
	0.0373	72	0.0478	4.78
	0.0379	96	0.0646	6.46
	0.0384	120	0.0787	7.87
	0.0386	144	0.0843	8.43
	0.0386	168	0.0843	8.43

M-LL-SIS-9.7-Mg

<b>W<sub>membrane after oven</sub> (g)</b>	<b>W<sub>wet membrane</sub> (g)</b>	<b>t (hr)</b>	<b>Water Swelling Ratio</b>	<b>%</b>
0.0338	0.0338	0	0.0000	0.00
	0.0362	72	0.0710	7.10
	0.0368	96	0.0888	8.88
	0.0374	120	0.1065	10.65
	0.0376	144	0.1124	11.24
	0.0376	168	0.1124	11.24

M-LL-SIS-14.3

<b>W<sub>membrane after oven</sub> (g)</b>	<b>W<sub>wet membrane</sub> (g)</b>	<b>t (hr)</b>	<b>Water Swelling Ratio</b>	<b>%</b>
0.0206	0.0206	0	0.0000	0.00
	0.0222	72	0.0777	7.77
	0.0225	96	0.0922	9.22
	0.0227	120	0.1019	10.19
	0.0227	144	0.1019	10.19
	0.0227	168	0.1019	10.19

M-LL-SIS-14.3-Ca

<b>W<sub>membrane after oven</sub> (g)</b>	<b>W<sub>wet membrane</sub> (g)</b>	<b>t (hr)</b>	<b>Water Swelling Ratio</b>	<b>%</b>
0.0180	0.018	0	0.0000	0.00
	0.0197	72	0.0944	9.44
	0.0200	96	0.1111	11.11
	0.0203	120	0.1278	12.78
	0.0205	144	0.1389	13.89
	0.0205	168	0.1389	13.89

M-LL-SIS-14.3-Ba

<b>W<sub>membrane after oven</sub> (g)</b>	<b>W<sub>wet membrane</sub> (g)</b>	<b>t (hr)</b>	<b>Water Swelling Ratio</b>	<b>%</b>
0.0242	0.0242	0	0.0000	0.00
	0.026	72	0.0744	7.44
	0.0265	96	0.0950	9.50
	0.0269	120	0.1116	11.16
	0.0271	144	0.1198	11.98
	0.0271	168	0.1198	11.98

M-LL-SIS-14.3-Mg

<b>W<sub>membrane after oven</sub> (g)</b>	<b>W<sub>wet membrane</sub> (g)</b>	<b>t (hr)</b>	<b>Water Swelling Ratio</b>	<b>%</b>
0.0308	0.0308	0	0.0000	0.00
	0.0329	72	0.0682	6.82
	0.0333	96	0.0812	8.12
	0.0335	120	0.0877	8.77
	0.0335	144	0.0877	8.77
	0.0335	168	0.0877	8.77

M-BL-SIS-12.6

<b>W<sub>membrane after oven</sub> (g)</b>	<b>W<sub>wet membrane</sub> (g)</b>	<b>t (hr)</b>	<b>Water Swelling Ratio</b>	<b>%</b>
0.0337	0.0337	0	0.0000	0.00
	0.0373	72	0.1068	10.68
	0.0379	96	0.1246	12.46
	0.0386	120	0.1454	14.54
	0.0389	144	0.1543	15.43
	0.0389	168	0.1543	15.43

M-BL-SIS-12.6-Ca

<b>W<sub>membrane after oven</sub> (g)</b>	<b>W<sub>wet membrane</sub> (g)</b>	<b>t (hr)</b>	<b>Water Swelling Ratio</b>	<b>%</b>
0.0325	0.0325	0	0.0000	0.00
	0.0359	72	0.1046	10.46
	0.0373	96	0.1477	14.77
	0.0376	120	0.1569	15.69
	0.0377	144	0.1600	16.00
	0.0377	168	0.1600	16.00

M-BL-SIS-12.6-Ba

<b>W<sub>membrane after oven</sub> (g)</b>	<b>W<sub>wet membrane</sub> (g)</b>	<b>t (hr)</b>	<b>Water Swelling Ratio</b>	<b>%</b>
0.0248	0.0248	0	0.0000	0.0000
	0.0272	72	0.0968	9.6774
	0.0279	96	0.1250	12.5000
	0.0285	120	0.1492	14.9194
	0.0287	144	0.1573	15.7258
	0.0287	168	0.1573	15.7258

M-BL-SIS-12.6-Mg

<b>W<sub>membrane after oven</sub> (g)</b>	<b>W<sub>wet membrane</sub> (g)</b>	<b>t (hr)</b>	<b>Water Swelling Ratio</b>	<b>%</b>
0.0197	0.0197	0	0.0000	0.00
	0.0218	72	0.1066	10.66
	0.0224	96	0.1371	13.71
	0.0228	120	0.1574	15.74
	0.0230	144	0.1675	16.75
	0.0230	168	0.1675	16.75

M-BL-SIS-23.3

<b>W<sub>membrane after oven</sub> (g)</b>	<b>W<sub>wet membrane</sub> (g)</b>	<b>t (hr)</b>	<b>Water Swelling Ratio</b>	<b>%</b>
0.0266	0.0266	0	0.0000	0.00
	0.0296	72	0.1128	11.28
	0.0300	96	0.1278	12.78
	0.0303	120	0.1391	13.91
	0.0304	144	0.1429	14.29
	0.0304	168	0.1429	14.29

M-BL-SIS-23.3-Ca

<b>W<sub>membrane after oven</sub> (g)</b>	<b>W<sub>wet membrane</sub> (g)</b>	<b>t (hr)</b>	<b>Water Swelling Ratio</b>	<b>%</b>
0.0190	0.0190	0	0.0000	0.00
	0.0208	72	0.0947	9.47
	0.0211	96	0.1105	11.05
	0.0213	120	0.1211	12.11
	0.0214	144	0.1263	12.63
	0.0214	168	0.1263	12.63

M-BL-SIS-23.3-Ba

<b>W<sub>membrane after oven</sub> (g)</b>	<b>W<sub>wet membrane</sub> (g)</b>	<b>t (hr)</b>	<b>Water Swelling Ratio</b>	<b>%</b>
0.0234	0.0234	0	0.0000	0.00
	0.0252	72	0.0769	7.69
	0.0258	96	0.1026	10.26
	0.0260	120	0.1111	11.11
	0.0260	144	0.1111	11.11
	0.0260	168	0.1111	11.11

M-BL-SIS-23.3-Mg

<b>W</b> membrane after oven (g)	<b>W</b> wet membrane (g)	<b>t</b> (hr)	<b>Water Swelling Ratio</b>	<b>%</b>
0.0221	0.0221	0	0.0000	0.00
	0.0251	72	0.1357	13.57
	0.0260	96	0.1765	17.65
	0.0266	120	0.2036	20.36
	0.0269	144	0.2172	21.72
	0.0269	168	0.2172	21.72

# Appendix D

## D.1 DMMP Vapor Transport Data

M-LL-SIS-9.7

Weight (g)	Time (hr)
21.8568	0
21.8474	23.5
21.8280	46.5
21.8242	70
21.8140	90

Slope (m)	T (°C)	D (m)	L (m)	A (m <sup>2</sup> )	VTR (gr/m <sup>2</sup> hr)	P1 (mmHg)	P2 (mmHg)	R	M	P <sub>eff</sub>
-0.0005	35.7	0.006	0.0003	2.8E-05	17.6928	7.11	0	0.0624	124.08	1.2E-04

M-LL-SIS-9.7-Ca

Weight (g)	Time (hr)
21.8683	0
21.8568	23.5
21.8376	46.5
21.8318	70
21.8198	90

Slope (m)	T (°C)	D (m)	L (m)	A (m <sup>2</sup> )	VTR (gr/m <sup>2</sup> hr)	P sat (mmHg)	P2 (mmHg)	R	M	P <sub>eff</sub>
-0.0005	35.7	0.006	0.0003	2.8E-05	17.6928	7.11	0	0.0624	124.08	1.2E-04

M-LL-SIS-9.7-Ba

Weight (g)	Time (hr)
21.9587	0
21.9334	23.5
21.8821	46.5
21.8699	70
21.8399	90

Slope (m)	T (°C)	D (m)	L (m)	A (m <sup>2</sup> )	VTR (gr/m <sup>2</sup> hr)	P sat (mmHg)	P2 (mmHg)	R	M	Peff
-0.0013	35.7	0.006	0.0003	2.8E-05	46.0014	7.11	0	0.0624	124.08	3.0E-04

M-LL-SIS-9.7-Mg

Weight (g)	Time (hr)
21.8645	0
21.8564	23.5
21.8438	46.5
21.8242	70
21.7784	90

Slope (m)	T (°C)	D (m)	L (m)	A (m <sup>2</sup> )	VTR (gr/m <sup>2</sup> hr)	P sat (mmHg)	P2 (mmHg)	R	M	Peff
-0.0009	35.7	0.006	0.0003	2.8E-05	31.8471	7.11	0	0.0624	124.08	2.1E-04

M-LL-SIS-14.3

Weight (g)	Time (hr)
22.7906	0
22.7572	23.5
22.6814	46.5
22.6652	70
22.6260	90

Slope (m)	T (°C)	D (m)	L (m)	A (m <sup>2</sup> )	VTR (gr/m <sup>2</sup> hr)	P sat (mmHg)	P2 (mmHg)	R	M	Peff
-0.0019	35.7	0.006	0.0003	2.8E-05	67.232838	7.11	0	0.0624	124.08	4.4E-04

M-LL-SIS-14.3-Ca

Weight (g)	Time (hr)
22.7162	0
22.6855	23.5
22.6131	46.5
22.5976	70
22.5601	90

Slope (m)	T (°C)	D (m)	L (m)	A (m <sup>2</sup> )	VTR (gr/m <sup>2</sup> hr)	P sat (mmHg)	P2 (mmHg)	R	M	Peff
-0.0018	35.7	0.006	0.0003	2.8E-05	63.6943	7.11	0	0.0624	124.08	4.2E-04

M-LL-SIS-14.3-Ba

Weight (g)	Time (hr)
22.3822	0
22.3352	23.5
22.2299	46.5
22.2073	70
22.1497	90

Slope (m)	T (°C)	D (m)	L (m)	A (m <sup>2</sup> )	VTR (gr/m <sup>2</sup> hr)	P sat (mmHg)	P2 (mmHg)	R	M	Peff
-0.0026	35.7	0.006	0.0003	2.8E-05	92.0028	7.11	0	0.0624	124.08	6.0E-04

M-LL-SIS-14.3-Mg

Weight (g)	Time (hr)
22.5692	0
22.5566	23.5
22.5268	46.5
22.5184	70
22.4992	90

Slope (m)	T (°C)	D (m)	L (m)	A (m <sup>2</sup> )	VTR (gr/m <sup>2</sup> hr)	P sat (mmHg)	P2 (mmHg)	R	M	Peff
-0.0008	35.7	0.006	0.0003	2.8E-05	28.3086	7.11	0	0.0624	124.08	1.9E-04

M-BL-SIS-12.6

Weight (g)	Time (hr)
22.5382	0
22.5141	23.5
22.4713	46.5
22.4625	70
22.4391	90

Slope (m)	T (°C)	D (m)	L (m)	A (m <sup>2</sup> )	VTR (gr/m <sup>2</sup> hr)	P sat (mmHg)	P2 (mmHg)	R	M	Peff
-0.0011	35.7	0.006	0.0003	2.8E-05	38.9243	7.11	0	0.0624	124.08	2.5E-04

M-BL-SIS-12.6-Ca

Weight (g)	Time (hr)
21.9824	0
21.9735	23.5
21.9558	46.5
21.9515	70
21.9413	90

Slope (m)	T (°C)	D (m)	L (m)	A (m <sup>2</sup> )	VTR (gr/m <sup>2</sup> hr)	P sat (mmHg)	P2 (mmHg)	R	M	Peff
-0.0005	35.7	0.006	0.0003	2.8E-05	17.6928	7.11	0	0.0624	124.08	1.2E-04

M-BL-SIS-12.6-Ba

Weight (g)	Time (hr)
21.7430	0
21.7304	23.5
21.7080	46.5
21.7018	70
21.6861	90

Slope (m)	T (°C)	D (m)	L (m)	A (m <sup>2</sup> )	VTR (gr/m <sup>2</sup> hr)	P sat (mmHg)	P2 (mmHg)	R	M	Peff
-0.0006	35.7	0.006	0.0003	2.8E-05	21.2314	7.11	0	0.0624	124.08	1.4E-04

M-BL-SIS-12.6-Mg

Weight (g)	Time (hr)
22.0368	0
22.0243	23.5
22.0051	46.5
22.0008	70
21.9903	90

Slope (m)	T (°C)	D (m)	L (m)	A (m <sup>2</sup> )	VTR (gr/m <sup>2</sup> hr)	P sat (mmHg)	P2 (mmHg)	R	M	Pe <sub>ff</sub>
-0.0005	35.7	0.006	0.0003	2.8E-05	17.6928	7.11	0	0.0624	124.08	1.2E-04

M-BL-SIS-23.3

Weight (g)	Time (hr)
22.5629	0
22.5521	23.5
22.5285	46.5
22.5231	70
22.5100	90

Slope (m)	T (°C)	D (m)	L (m)	A (m <sup>2</sup> )	VTR (gr/m <sup>2</sup> hr)	P sat (mmHg)	P2 (mmHg)	R	M	Pe <sub>ff</sub>
-0.0006	35.7	0.006	0.0003	2.8E-05	21.2314	7.11	0	0.0624	124.08	1.4E-04

M-BL-SIS-23.3-Ca

Weight (g)	Time (hr)
22.8964	0
22.8855	23.5
22.8654	46.5
22.8597	70
22.8469	90

Slope (m)	T (°C)	D (m)	L (m)	A (m <sup>2</sup> )	VTR (gr/m <sup>2</sup> hr)	P sat (mmHg)	P2 (mmHg)	R	M	Pe <sub>ff</sub>
-0.0006	35.7	0.006	0.0003	2.8E-05	21.2314	7.11	0	0.0624	124.08	1.4E-04

M-BL-SIS-23.3-Ba

Weight (g)	Time (hr)
22.1645	0
22.1553	23.5
22.1390	46.5
22.1340	70
22.1241	90

Slope (m)	T (°C)	D (m)	L (m)	A (m <sup>2</sup> )	VTR (gr/m <sup>2</sup> hr)	P sat (mmHg)	P2 (mmHg)	R	M	Pe <sub>eff</sub>
-0.0005	35.7	0.006	0.0003	2.8E-05	17.6928	7.11	0	0.0624	124.08	1.2E-04

M-BL-SIS-23.3-Mg

Weight (g)	Time (hr)
21.9234	0
21.9015	23.5
21.8536	46.5
21.8417	70
21.8131	90

Slope (m)	T (°C)	D (m)	L (m)	A (m <sup>2</sup> )	VTR (gr/m <sup>2</sup> hr)	P sat (mmHg)	P2 (mmHg)	R	M	Pe <sub>eff</sub>
-0.0012	35.7	0.006	0.0003	2.8E-05	42.4628	7.11	0	0.0624	124.08	2.8E-04

## D.2 Water Vapor Transport Data

M-LL-SIS-9.7

Weight (g)	Time (hr)
21.0688	24
21.0609	47.5
21.0566	72.5
21.0558	96
21.0552	120

Slope (m)	T (°C)	D (m)	L (m)	A (m <sup>2</sup> )	VTR (gr/m <sup>2</sup> hr)	P1 (mmHg)	P2 (mmHg)	R	M	Pe <sub>eff</sub>
-0.0001	35.1	0.006	0.0003	2.8E-05	3.5386	41.175	0	0.0624	18	3.0E-05

M-LL-SIS-9.7-Ca

Weight (g)	Time (hr)
21.5029	24
21.4977	47.5
21.4973	72.5
21.4964	96
21.4945	120

Slope (m)	T (°C)	D (m)	L (m)	A (m <sup>2</sup> )	VTR (gr/m <sup>2</sup> hr)	P sat (mmHg)	P2 (mmHg)	R	M	P <sub>eff</sub>
-0.00007	35.1	0.006	0.0003	2.8E-05	2.4770	41.175	0	0.0624	18	1.9E-05

M-LL-SIS-9.7-Ba

Weight (g)	Time (hr)
21.2682	24
21.2192	47.5
21.1997	72.5
21.1978	96
21.1868	120

Slope (m)	T (°C)	D (m)	L (m)	A (m <sup>2</sup> )	VTR (gr/m <sup>2</sup> hr)	P sat (mmHg)	P2 (mmHg)	R	M	P <sub>eff</sub>
-0.0008	35.1	0.006	0.0003	2.8E-05	28.3086	41.175	0	0.0624	18	2.2E-04

M-LL-SIS-9.7-Mg

Weight (g)	Time (hr)
21.5529	24
21.5101	47.5
21.4932	72.5
21.4884	96
21.4532	120

Slope (m)	T (°C)	D (m)	L (m)	A (m <sup>2</sup> )	VTR (gr/m <sup>2</sup> hr)	P sat (mmHg)	P2 (mmHg)	R	M	P <sub>eff</sub>
-0.0009	35.1	0.006	0.0003	2.8E-05	31.8471	41.175	0	0.0624	18	2.5E-04

M-LL-SIS-14.3

Weight (g)	Time (hr)
21.1902	24
20.9332	47.5
20.8766	72.5
20.8607	96
20.8132	120

Slope (m)	T (°C)	D (m)	L (m)	A (m <sup>2</sup> )	VTR (gr/m <sup>2</sup> hr)	P sat (mmHg)	P2 (mmHg)	R	M	Peff
-0.0016	35.1	0.006	0.0003	2.8E-05	56.6171	41.175	0	0.0624	18	4.4E-04

M-LL-SIS-14.3-Ca

Weight (g)	Time (hr)
21.5949	24
21.4861	47.5
21.4565	72.5
21.4499	96
21.4246	120

Slope (m)	T (°C)	D (m)	L (m)	A (m <sup>2</sup> )	VTR (gr/m <sup>2</sup> hr)	P sat (mmHg)	P2 (mmHg)	R	M	Peff
-0.0008	35.1	0.006	0.0003	2.8E-05	28.3086	41.175	0	0.0624	18	2.2E-04

M-LL-SIS-14.3-Ba

Weight (g)	Time (hr)
21.3232	24
21.1371	47.5
21.0931	72.5
21.0821	96
21.0482	120

Slope (m)	T (°C)	D (m)	L (m)	A (m <sup>2</sup> )	VTR (gr/m <sup>2</sup> hr)	P sat (mmHg)	P2 (mmHg)	R	M	Peff
-0.0012	35.1	0.006	0.0003	2.8E-05	42.4628	41.175	0	0.0624	18	3.3E-04

M-LL-SIS-14.3-Mg

Weight (g)	Time (hr)
21.4540	24
21.3622	47.5
21.3290	72.5
21.3193	96
21.2923	120

Slope (m)	T (°C)	D (m)	L (m)	A (m <sup>2</sup> )	VTR (gr/m <sup>2</sup> hr)	P sat (mmHg)	P2 (mmHg)	R	M	Peff
-0.0009	35.1	0.006	0.0003	2.8E-05	31.8471	41.175	0	0.0624	18	2.5E-04

M-BL-SIS-12.6

Weight (g)	Time (hr)
21.5345	24
21.4583	47.5
21.4403	72.5
21.4385	96
21.4221	120

Slope (m)	T (°C)	D (m)	L (m)	A (m <sup>2</sup> )	VTR (gr/m <sup>2</sup> hr)	P sat (mmHg)	P2 (mmHg)	R	M	Peff
-0.0005	35.1	0.006	0.0003	2.8E-05	17.6928	41.175	0	0.0624	18	1.4E-04

M-BL-SIS-12.6-Ca

Weight (g)	Time (hr)
21.5624	24
21.5561	47.5
21.5539	72.5
21.5570	96
21.5548	120

Slope (m)	T (°C)	D (m)	L (m)	A (m <sup>2</sup> )	VTR (gr/m <sup>2</sup> hr)	P sat (mmHg)	P2 (mmHg)	R	M	Peff
-0.00006	35.1	0.006	0.0003	2.8E-05	2.1231	41.175	0	0.0624	18	1.6E-05

M-BL-SIS-12.6-Ba

Weight (g)	Time (hr)
21.4480	24
21.4331	47.5
21.4282	72.5
21.4308	96
21.4238	120

Slope (m)	T (°C)	D (m)	L (m)	A (m <sup>2</sup> )	VTR (gr/m <sup>2</sup> hr)	P sat (mmHg)	P2 (mmHg)	R	M	Peff
-0.0002	35.1	0.006	0.0003	2.8E-05	7.0771	41.175	0	0.0624	18	5.5E-05

M-BL-SIS-12.6-Mg

Weight (g)	Time (hr)
21.4692	24
21.4687	47.5
21.4672	72.5
21.4696	96
21.4691	120

Slope (m)	T (°C)	D (m)	L (m)	A (m <sup>2</sup> )	VTR (gr/m <sup>2</sup> hr)	P sat (mmHg)	P2 (mmHg)	R	M	Peff
-0.00004	35.1	0.006	0.0003	2.8E-05	1.4154	41.175	0	0.0624	18	1.1E-05

M-BL-SIS-23.3

Weight (g)	Time (hr)
21.0688	24
21.0613	47.5
21.0582	72.5
21.0572	96
21.0560	120

Slope (m)	T (°C)	D (m)	L (m)	A (m <sup>2</sup> )	VTR (gr/m <sup>2</sup> hr)	P sat (mmHg)	P2 (mmHg)	R	M	Peff
-0.0001	35.1	0.006	0.0003	2.8E-05	3.5386	41.175	0	0.0624	18	2.7E-05

M-BL-SIS-23.3-Ca

Weight (g)	Time (hr)
21.6332	24
21.5972	47.5
21.5849	72.5
21.5821	96
21.5705	120

Slope (m)	T (°C)	D (m)	L (m)	A (m <sup>2</sup> )	VTR (gr/m <sup>2</sup> hr)	P sat (mmHg)	P2 (mmHg)	R	M	Peff
-0.0006	35.1	0.006	0.0003	2.8E-05	21.2314	41.175	0	0.0624	18	1.6E-04

M-BL-SIS-23.3-Ba

Weight (g)	Time (hr)
21.3883	24
21.3332	47.5
21.3206	72.5
21.3197	96
21.3058	120

Slope (m)	T (°C)	D (m)	L (m)	A (m <sup>2</sup> )	VTR (gr/m <sup>2</sup> hr)	P sat (mmHg)	P2 (mmHg)	R	M	Peff
-0.0007	35.1	0.006	0.0003	2.8E-05	24.7670	41.175	0	0.0624	18	1.9E-04

M-BL-SIS-23.3-Mg

Weight (g)	Time (hr)
21.9234	0
21.9015	23.5
21.8536	46.5
21.8417	70
21.8131	90

Slope (m)	T (°C)	D (m)	L (m)	A (m <sup>2</sup> )	VTR (gr/m <sup>2</sup> hr)	P sat (mmHg)	P2 (mmHg)	R	M	Peff
-0.0008	35.1	0.006	0.0003	2.8E-05	28.3086	41.175	0	0.0624	18	2.2E-04

# Appendix E

## E.1 SAXS curves used to calculate the Bragg distance

